AIR FORCE INSTITUTE OF TECHNOLOGY

AIR UNIVERSITY
UNITED STATES AIR FORCE

by

Robert Charles Geiss, B.S.

Captain USAF

Graduate Astronautics

SCHOOL OF ENGINEERING

WRIGHT-PATTERSON AIR FORCE BASE, OHIO

AF-WP-O-MAY 62 3,500

AN INVESTIGATION OF DIFFUSION IN THE COLUMBIUM VANADIUM SYSTEM

THESIS

Presented to the Faculty of the School of Engineering of
the Air Force Institute of Technology
Air University
in Partial Fulfillment of the
Requirements for the Degree of
Master of Science

by

Robert Charles Geiss, B.S.
Captain USAF
Graduate Astronautics

August 1962

Preface

This study was a result of a request by the High Temperature Metals Section, Directorate of Materials and Processes, Aeronautical Systems Division, for a study on diffusion rates in the refractory metals system of columbium and vanadium.

The author would like to thank Major (then Captain) E. J. Myers of the AFIT Mechanics Department for his valuable criticisms and his admirable knack of keeping hands-off my work, thus letting me make my own mistakes. I am deeply indebted to Mr. (then Lt.) Craig Hartley of the High Temperature Metals Section for his patience, fortitude, and vast technical metallurgical background. I wish to thank the various personnel of the High Temperature Metals Section for their cooperation and forbearance, particularly during those trying weeks when furnaces and specimens were suffering catastrophic failures with blood-chilling regularity. I am indebted to Mr. Kenneth Hubbard of the Programming Branch, Digital Computer Section, ASD, for his help and cooperation above and beyond the mere call of duty in ironing out the wrinkles in the computer program. His day and night work and interest enabled this thesis to be completed on time.

Finally, I would like to express appreciation to

my family - - who never could understand what <u>all</u> the fuss and furor was about. In retrospect, I can't either.

Robert C. Geiss

GA/Mech 62-2

Abstract

Diffusion rates in the Cb-V system were investigated using electron microprobe analysis of the diffusion zones to determine concentration gradients. The interdiffusion coefficient, D, was found using a computer program to solve the Matano-Boltzman method. Activation energies, Q, and frequency factors, D_o, were derived from values of D at the same concentrations but at different temperatures.

A partial list of D_o and Q for interdiffusion (in lattice parameter measure) as a function of composition is:

5 a/o Cb; Q = 59.8 Kcal/mol, D_o = 5.3x

55 a/o Cb; Q = 48.1 Kcal/mol, D_o = 9.5x

95 a/o Cb; Q = 69.4 Kcal/mol, D_o = 7.0x

Movement of tungsten Kirkendall markers at 12.7 a/o Cb and 1404°C. during the diffusion anneal indicated $D_V > D_{Cb}$.

Diffusion in the Cb-V system is apparently by a vacancy mechanism.

R- ix

Contents

my family - - who never could understand what <u>all</u> the fuss and furor was about. In retrospect, I can't either.

Robert C. Geiss

Contents

List of Figures

List of Figures (Cont'd)

List of Tables

Abstract

Diffusion rates in the Cb-V system were investigated using electron microprobe analysis of the diffusion zones to determine concentration gradients. The interdiffusion coefficient, D, was found using a computer program to solve the Matano-Boltzman method. Activation energies, Q, and frequency factors, D_o, were derived from values of D at the same concentrations but at different temperatures.

A partial list of D_o and Q for interdiffusion (in lattice parameter measure) as a function of composition is:

5 a/o Cb; Q = 59.8 Kcal/mol, $D_o = 5.3 \times 10^{16} lp^2/hr$

55 a/o Cb; Q = 48.1 Kcal/mol, $D_o = 9.5 \times 10^{14} lp^2/hr$

95 a/o Cb; Q = 69.4 Kcal/mol, $D_o = 7.0 \times 10^{15} lp^2/hr$

Movement of tungsten Kirkendall markers at 12.7 a/o Cb and 1404°C. during the diffusion anneal indicated $D_V > D_{Cb}$.

Diffusion in the Cb-V system is apparently by a vacancy mechanism.

BLANK PAGE

I. Introduction

The rates of diffusion in refractory metals have become increasingly important in the past few years. Diffusion mechanisms largely control rates of creep, oxidation, age-hardening, sintering, and homogenization in all metals. Most reactions in the solid state are greatly dependent on the diffusion of atoms along grain boundaries, through surfaces, and through the lattice structures themselves. It is the last of the types of diffusion, normally called volume or bulk diffusion, that the author has investigated with respect to the columbium-vanadium binary system. Volume diffusion can further be subdivided into three different regimes: the diffusion of substitutional atoms into the parent metal lattice; interstitial diffusion, which is the description of motion of atoms within the interstices of the metallic lattice; and self diffusion which is the movement of atoms of a given kind in their own crystal lattice. (Refs 13; 25). Relative atom size of the two metals under consideration ruled out the likelihood of any appreciable interstitial diffusion between them.

The low thermal neutron cross-sections, excellent corrosion resistant properties, and high temperature strengths of columbium and vanadium have prompted investigations of their use as nuclear cladding materials

or nuclear reactor structural components (Refs 21; 26). Therefore, the study of diffusion rates of columbium and vanadium has immediate applications in modern technology.

Scope

The subject of this thesis was an investigation of diffusion in the columbium-vanadium system using electron microbeam probe analysis to determine the concentration-penetration curves. The interdiffusion coefficient, D, was found using the Matano-Boltzman method for a variable D as a function of concentration. Activation energies, Q, and frequency factors, D_o, were derived from values of D at the same concentrations but at different diffusion temperatures. Attempts were also made to find the intrinsic diffusion coefficients, D_{Cb} and D_V, using Kirkendall markers to measure mass flows from original interface boundaries.

Since the columbium-vanadium binary system forms a continuous series of solid solutions, this diffusion investigation was not hampered by the formation of intermediate phases or intermetallic compounds. Both columbium and vanadium have body-centered cubic (bcc) crystal structures (Ref 11:1022).

Plan of Investigation

This independent study was divided into three experimental and investigative parts. The first, or preparatory, part was in two phases; one phase consisted of preparation of metallic standards for microbeam probe intensity calibration, and the other phase was devoted to a parallel preparation and diffusion heat treatment of the diffusion couples. The second part of this thesis was reduction of the concentration-penetration data furnished by the electron microbeam probe analysis across the various diffusion zones of the diffusion couples so that various values of D could be determined by iterative means employing a computer program. Finally, derived values for the diffusion coefficients, frequency factors, activation energies and intrinsic diffusion coefficients were catalogued, examined, and analyzed in an attempt to fit a diffusion mechanism to the observed diffusion in the columbium-vanadium system.

Format of Report

The general scheme of this report is as outlined in this paragraph. Section II is devoted to general theory and overall concepts of volume diffusion and some of the pertinent ramifications. Section III describes experimental

procedure in detail and some of the more useful general techniques employed. Section IV describes the results obtained from the electron probe analysis of the couples and computer values of diffusion coefficients are presented. Section V presents conclusions and general discussion of the results of Section IV and recommendations both for further work in the field and local equipment modifications. The Appendices describe in detail the electron microprobe techniques and theory, the X-ray analysis and density determinations of the microprobe standards, general equipment employed in the diffusion anneals, and computer techniques used in diffusivity calculations.

II. Theory

General

Diffusion in metals is mass flow due to random atomic movement under a driving force of a difference in free energy from one region in the crystal lattice to another. The theoretical work of Fick, published in 1855 and based on Fourier's mathematical equation of heat conduction, is held to be the descriptive basis for diffusion theory. Assuming an isothermal, isotropic, isobaric binary system, Fick's first law states that the amount of diffusing substance, J, which passes through unit area of a plane perpendicular to the direction of diffusion in unit time is proportional to the concentration gradient of the diffusing substance. Considering diffusion to be one-dimensional for simplicity of analysis and the x-direction as the direction of diffusion, we have:

$$J = -D \left(\frac{\partial C}{\partial X}\right) \qquad (1)$$

where $\partial C/\partial x$ is the concentration gradient of diffusing substance in the x-direction, C is concentration in moles per unit volume and is a function of x across the diffusion zone. D, the diffusivity or diffusion coefficient, is written as a proportionality factor and has the units of distance^2 / time. D is considered a function of C in this paper as this form of the

differential equation is considered most applicable to interdiffusing metals (Ref 18:309).

Applying the conservation of mass across a given volume element enables Fick's second law to be derived from the first:

$$\partial C/\partial t = \frac{\partial}{\partial x}\left(D\frac{\partial C}{\partial x}\right) \qquad (2)$$

where t is diffusion time, C is concentration and x is again the diffusion direction coordinate (Ref 8: 1.2, 1.3).

Matano Method of Determining D

The concept of a diffusion coefficient that varies with composition was first used by Matano. He applied a mathematical solution of Boltzman to (2) using the substitution $\lambda = x/\sqrt{t}$, based on the empirical observation that x^2 is proportional to t at any given C (Ref 20:109). Thus C is a function of λ, and the solution of (2) becomes:

$$D = -\left(\frac{1}{2t}\right)\left(\frac{\partial C}{\partial x}\right)^{-1}\int_{C_A}^{C_x} x\, dC \qquad (3)$$

for a given t and the boundary conditions:

$t = 0$ $\quad C = C_o, \quad x < 0$
$\quad\quad\quad\quad C = C_i, \quad x > 0$

$t > 0$ $\quad dC/dx = 0, \; C = C_o,$

GA/MECH 62-2

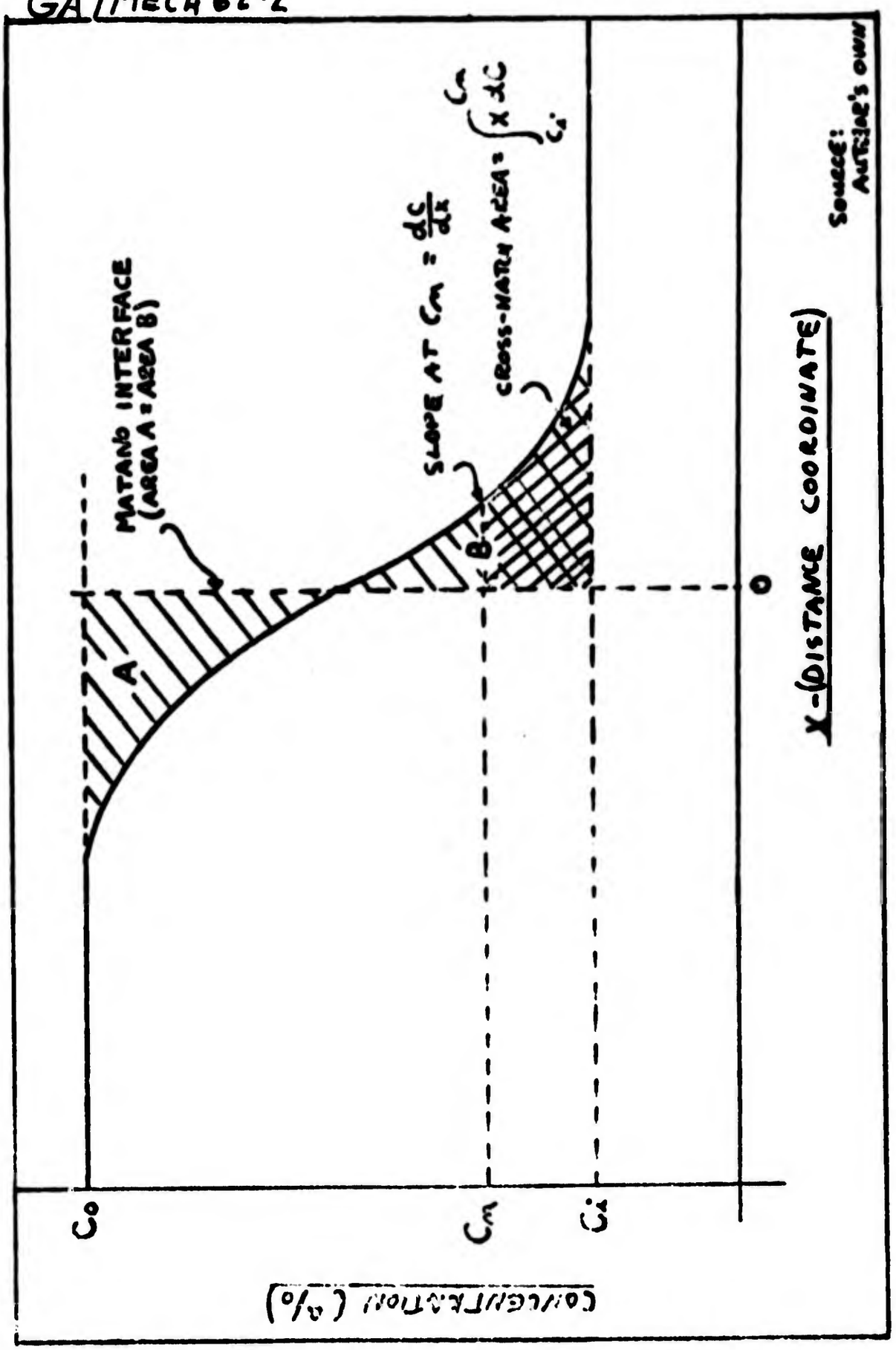

Figure 1 - Typical Concentration Gradient Profile Showing dC/dx, the Matano Interface, and $\int_{C_i}^{C_o} x\,dC$.

BLANK PAGE

and where the origin coordinates satisfy the relation:

$$\int_{C_4}^{C_0} x \, dC = 0 \text{ (Ref 2:47-49).}$$

Thus, (3) defines the diffusivity, D, at composition C_n. The origin is commonly referred to as the Matano interface. The Matano interface, dC/dx, and $\int x \, dC$ are illustrated in Figure 1. Values of D as a function of C can then be determined from the concentration-penetration curve for a given temperature and time by iterative means using a technique such as Simpson's Rule to evaluate the integral (Ref 8:232-233). The mechanics of the techniques used in this report to find D as a function of C for the columbium-vanadium system investigated are described in Appendix D of this report. The Matano interface, x_M, is fixed at the original interface at t>0 only if there is no volume change during diffusion.

Intrinsic Diffusion Coefficients

For years it was assumed that a single diffusion coefficient, D, was sufficient to describe diffusion at a constant temperature for a given concentration. However, certain experimenters as early as 1933 found evidence that diffusion rates for the components of a binary system were unequal (Ref 14:799).

In general, for the atoms of components A and B, differences in their respective mobilities due to

differences in their masses, sizes, or activities would result in the random motion transfer of A to be greater or less than B across a fixed section. As a result, a pressure would tend to build up in the region that added less to the rate of transfer. This pressure is relieved by resultant mass flow of A and B into the more active region. The overall rate of transfer of one component (say B) must then be described as the effect of both true diffusion (random atomic motion of non-uniformly distributed B atoms) and the pressure compensating mass flow of both A and B. Diffusion interpretation by means of the single diffusion coefficient D would be complicated and masked by this mass flow.

Therefore, new diffusion coefficients, D_A and D_B, were defined in terms of the respective transfer rates of A and B across a section fixed so that no mass flow occurs through it (Ref 8:225-226). These coefficients were called the intrinsic diffusion coefficients.

Theoretically, interest lay mainly in the diffusion of atoms past a given reference point in a crystal lattice. Therefore, some means had to be devised that would experimentally observe the mass flow of the lattice so that the diffusion effects could be compared to the reference points. Lattice point observation

is nigh impossible at best, so the alternative was to insert inert markers into diffusion specimens which would remain fixed relative to the lattice and therefore share its mass flow motion, yet not take part in any diffusion process. These markers are called Kirkendall markers and their movement is called the Kirkendall effect. The experimental work of Kirkendall and Smigelkas showed that the markers moved according to the parabolic law:

$$x_m = b\sqrt{t} \tag{4}$$

where x_m is the position of the marker interface, t is time, and b a proportionality constant (Ref 16). Therefore:

$$V_m = d\,x_m/dt = b/2\sqrt{t} = x_m/2t \tag{5}$$

where V_m is the velocity of the marker in distance/time.

The flow of A and B atoms per unit time per unit area across the marker interface then may be expressed as follows:

$$d\,n_A/dt = -\left(D_A \frac{\partial C_A}{\partial x} - C_A V_m\right) \tag{6}$$

and similarly:

$$d\,n_B/dt = -\left(D_B \frac{\partial C_B}{\partial x} - C_B V_m\right) \tag{7}$$

where $d\,n_A/dt$ and $d\,n_B/dt$ are atom fluxes of A and B, D_A and D_B are intrinsic diffusion coefficients of A and B, C_A and C_B are concentrations of A and B in atoms per

unit volume, x is the distance coordinate in the diffusion direction, and V_m is as derived in (5) and is distance/time.

Applying Fick's second law (2) to (6) and (7) yields:

$$\partial C_A/\partial t = \frac{\partial}{\partial x}\left(D_A \frac{\partial C_A}{\partial x} - C_A V_m\right) = \frac{\partial}{\partial x}\left(D \frac{\partial C_A}{\partial x}\right) \quad (8)$$

$$\partial C_B/\partial t = \frac{\partial}{\partial x}\left(D_B \frac{\partial C_B}{\partial x} - C_B V_m\right) = \frac{\partial}{\partial x}\left(D \frac{\partial C_B}{\partial x}\right) \quad (9)$$

Since $C_A + C_B = C$ (constant) for all x in the diffusion direction, the sum of (8) and (9) is:

$$\frac{\partial (C_A + C_B)}{\partial t} = 0 = \frac{\partial}{\partial x}\left(D_A \frac{\partial C_A}{\partial x} + D_B \frac{\partial C_B}{\partial x} - C V_m\right) \quad (10)$$

which integrates to:

$$D_A \frac{\partial C_A}{\partial x} + D_B \frac{\partial C_B}{\partial x} - C V_m = K. \quad (11)$$

But the boundary conditions at $x = \pm\infty$ are that $\partial C_B/\partial x = -\partial C_A/\partial x = 0$. Therefore, K=0 and:

$$V_m = \frac{1}{C}\left(D_A \frac{\partial C_A}{\partial x} + D_B \frac{\partial C_B}{\partial x}\right) \quad (12)$$

Letting N_A be the atom fraction of A (C_A/C), and noting that $\partial C_A/\partial x = -\partial C_B/\partial x$, we have:

$$(D_A - D_B) \frac{\partial N_A}{\partial x} = V_m \quad (13)$$

Plugging (13) into (8) yields:

$$\partial C_A/\partial t = \frac{\partial}{\partial x}\left(D \frac{\partial C_A}{\partial x}\right) = \frac{\partial}{\partial x}\left(\left[D_A (1-N_A) + D_B N_A\right] \frac{\partial C_A}{\partial x}\right) \quad (14)$$

Therefore,

$$D = D_A (1 - N_A) + D_B N_A \tag{15}$$

or:

$$D = N_A D_B + N_B D_A \tag{16}$$

With the knowledge of V_m and D at the marker interface, it is possible to solve for D_A and D_B at the compositions corresponding to the marker position by simultaneous solution of (15) and (13).

Temperature Dependence of D

The variations of diffusion coefficient with temperature is normally written in the form of an Arrhenius equation:

$$D = D_o \, e^{-Q/RT} \tag{17}$$

where D is the diffusion coefficient, D_o is the frequency factor (sometimes referred to as the diffusivity at infinite T), R is the gas constant, T is the absolute temperature, and Q is the activation energy for diffusion. For a given concentration (or composition), D_o and Q are approximately constant (Ref 15:215-232). A theoretical discussion is given in Section V on the values of D_o and Q derived from the experimental data of this thesis. It would seem reasonable to assume if the activation energies of the diffusing species are

dissimilar, a plot of log D versus 1/T (as commonly presented) would not necessarily plot as a straight line.

Molal Volume Change

The preceding arguments and derivations of diffusion coefficients have disregarded the possibility of molal volume changes with changing composition. In general, and in particular in this paper, this assumption is invalid as the molal volumes of columbium and vanadium differ appreciably (Table II). If the molal volume changes are ignored, the diffusion coefficients derived from the experimental data will be in error because, effectively, the number of atoms per unit volume of one component will not equal the number of atoms per unit volume of the other component at equivalent atomic percentages. Or, in the case of this paper, there will be more vanadium atoms per cubic centimeter that columbium atoms per cubic centimeter on their respective sides of the diffusion couple.

Several techniques have been proposed to correct for this source of error. Crank proposes two approximate solutions (Ref 8:236-240) and Baluffi offers an exact solution for D (Ref 1:872-873). However, another alternative, probably more attractive than either of those proposed above, is one in which distances and dimensions

are measured in lattice parameters rather than centimeters or inches. The use of lattice parameters automatically corrects for any molal volume changes that occur in the solid solutions (Ref 32:46). The X-ray determination of lattice parameters as a function of composition throughout the entire series of solid solutions of the columbium-vanadium system has been an integral part of this thesis. The parameter variations can be used not only in plotting and computing D values directly, but also can be used to determine molal volume changes with composition, if desired.

Activation Energy

The measure of the temperature dependence of the diffusion process is the activation energy (Q) which appears as one of the constants of (17). The activation energy is related to the energy that is required to force a diffusing atom past a low energy barrier point ("saddle point") in the atomic lattice. Since this energy involves the distortion and straining of atomic bonds, it is logical to try to correlate activation energy with quantities that indicate the strength of atomic bonding (Ref 25). For self diffusion, LeClaire (Ref 18:373) proposed the approximate relation:

$$Q = 38\ T_m \tag{19}$$

where T_m is the absolute melting temperature and Q is in calories/gram atom. Sherby and Simnad have attempted a quite involved empirical relationship where the activation energy for diffusion is related to melting temperature, crystal structure, and metallic "valence" in both dilute alloys and pure metals (Ref 28). They state:

$$D = D_o\, e^{\frac{-(K_o + V)\, T_m}{T}} \tag{20}$$

where D_o is a universal constant approximately 1 cm^2/sec, K_o is a crystal structure constant and equal to 14 for a bcc lattice, and V is a constant that depends rather haphazardly upon the chemical valence of the solute. For columbium, V is equal to about +3. No values were given for vanadium. D found from this relation fits empirical data fairly well for those systems where the valence of the solute can be determined.

TABLE I

Impurities in Cb and V Metals

(As Received Impurities by Weight)

Impurity	Vanadium Chips	Columbium Ingot
C	0.0480%	0.0155%
H	0.0100%	-------
O	0.0880%	0.0270%
N	0.0320%	0.0100%
Fe[1]	0.0010%	0.1000%
Si[1]	0.0100%	0.1000%
Mg[1]	0.0001%	0.0001%
Mn[1]	0.0010%	-------
Al[1]	0.0010%	0.0010%
Cu[1]	0.0010%	0.0010%

1- Analysis determined by Materials Central Spectrographic analysis. Other constituents are manufacturer's nominal values.

BLANK PAGE

III. Experimental Procedures

Standards Alloy Preparation

The vanadium used in the experimental portion of this paper was received in commercial high purity grade chip form. The columbium was received in the form of an ingot. Principal impurities are listed by weight analysis in Table I using the manufacturer's nominal analysis for gaseous impurities and the Aeronautical Systems Division, Directorate of Materials and Processes (Materials Central) spectrographic analysis for other impurities. Both metals were received from Mallory-Sharon Metals Corporation. The columbium ingot was turned down on a lathe, and the turnings were used in preparing the standards in conjunction with the vanadium chips. Nine 50-gram alloys were prepared to cover the composition range from 0 to 100 a/o (atomic percent) columbium in 10 to 15 a/o increments. The vanadium chips and the columbium turnings were weighed to the nearest hundredth of a gram and then compressed at 5000 psi pressure in a massive tool-steel die to compact the columbium turnings. Care was necessary because the chips and turnings were almost incompatible until compacted.

The compacted alloy mixtures were arc-melted at the University of Dayton Research Institute Metallurgy

Laboratory under Air Force contract. Private conversation held with Dr. Ray, head of the laboratory, on 1 December 1961 revealed that the procedures outlined in the following paragraph were used for each melt.

The compacts were placed on a water-cooled copper hearth and were arc-melted using a non-consumable tungsten electrode. Before each melt, the furnace chamber was evacuated to a pressure of 1 micron (10^{-3}mm Hg) and flushed to atmospheric pressure with a purified gas mixture of 75% argon - 25% helium. This procedure was repeated twice. Additionally, a titanium button was placed in the chamber as a "getter" to insure no reactive gasses were present during the melt. The getter button was melted before the standard compacts were melted. All melting was done under an argon-helium atmosphere at 350 mm Hg pressure. The procedure for each melt was to melt each alloy, turn it over, remelt the button, and repeat the operation until each alloy had been melted four to six times. Weight losses from 0.19% to 2.18% were noted for the various samples. These weight losses represented no subsequent data error because independent atomic percentage calculations were done after homogenization anneals using measured

GA/MECH 62-2

Figure 2- Specimen in evacuated hot-rolling "can". Ends are welded and vacuum access was through tube in upper left corner.

BLANK PAGE

lattice parameter and density data. The melted alloys were obtained as round, flat discs about $\frac{1}{4}$-inch thick and $1\frac{1}{4}$-inches in diameter.

Since the alloys were melted on a water cooled hearth, the alloys were subjected to very rapid non-equilibrium cooling from the molten to the solid state. The rapid cooling would prevent inter-diffusion and alloy homogenization. As a result, it was assumed that a cored structure existed in each standard - each core with a relatively high melting point composition surrounded by alloy of lower melting point - and homogenization of each specimen was needed.

The nine 50-gram buttons were then bright pickled in nitric acid, coated with an alumina powder slurry parting compound, and "canned" in stainless steel as a prelude to hot rolling operations. The cans were evacuated to 25 to 50 microns and sealed off (Figure 2). Since both vanadium and columbium exhibit severe oxidation tendencies at elevated temperatures, all subsequent hot-rolling and annealing operations were performed either under vacuum or an inert gas shield (Refs 21; 26).

Private conversations with personnel of the Battelle Memorial Institute Non-Ferrous Metallurgy Section

indicated that hot-rolling operations should be accomplished above 1000°C. Therefore, each can was heated to 1100°C. under an argon gas shield prior to being fed into the Materials Central rolling mill. After one pass of about 30% thickness reduction, three cans tore open with resultant localized oxidation of the inclosed alloy. Further hot-rolling operations were abandoned after one pass with each standard. The cans were allowed to air cool to room temperature before the standards were removed. When the alloys were placed into the cans, no attempt was made to have a tight fit of the specimens in the cans. Apparently, the rolls "grabbed" the cans during the start of the hot-roll. If the specimens were not aligned parallel to the rolls, the softened cans tore open as the alloys were forcibly aligned by the rolls during the pass. The three oxidized samples were trimmed on a cutting wheel and the small oxidized portions of each were discarded. All the standards were then bright pickled for 20 to 30 seconds in a mixture of two parts HNO_3, two parts H_2SO_4, and one part 52% HF.

All nine of the standards were annealed under a purified helium atmosphere at 1300°C. for 12 hours to complete homogenization. Each specimen was wrapped in tantalum foil and all were placed in a Marshall

GA/MECH 62-2

Figure 3- Grain structure of 21 a/o Cb standard after 12 hour homogenization anneal at 1300°C. Etchant 2 parts H_2SO_4, 2 parts HNO_3, 1 part 52% HF. 250X.

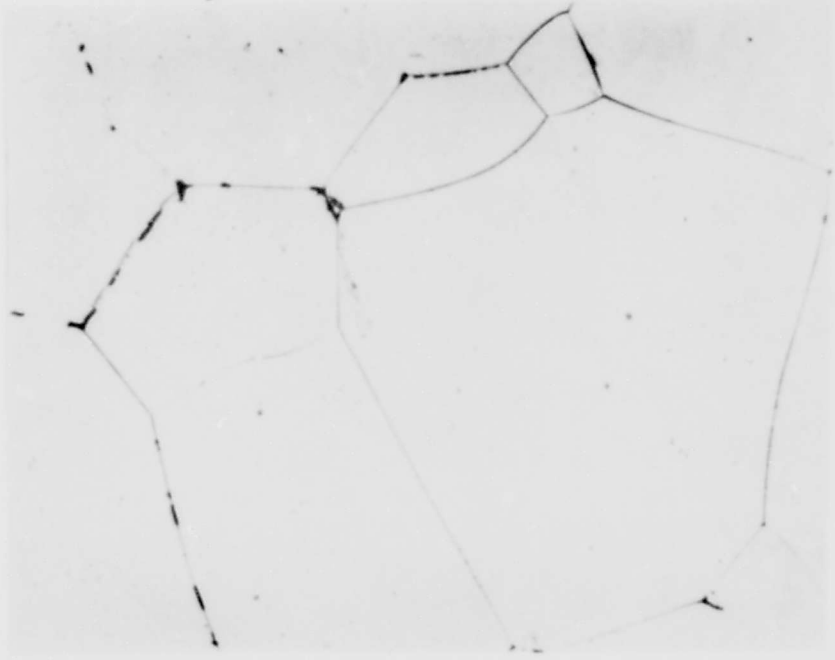

Figure 4- Grain structure of 72 a/o Cb standard after 12 hour homogenization anneal at 1300°C. Etchant 2 parts H_2SO_4, 2 parts HNO_3, 1 part 52% HF. 250X.

BLANK PAGE

furnace (Appendix B) at room temperature. The furnace was evacuated to 100 microns and heated to 800°C. at which temperature the purified helium gas was introduced into the system. Helium pressure slightly above atmospheric was maintained throughout the remainder of the run. Temperature was then brought to 1300°C. and held for 12 hours before power was turned off and the furnace allowed to cool. The tantalum foil was not embrittled and the standards looked clean when they were removed. Two samples in the as-annealed condition were mounted and examined metallographically at 250X (Figures 3 and 4). They showed uniform grain size and no apparent inhomogeneities. Also, the grain size was large enough so that bulk diffusion studies could be made without significant grain boundary diffusion effects. No further heat treatment was done on the standards. However, filings were taken from each specimen for x-ray lattice parameter measurement and each sample was also weighed in air and water for density determination.

Accurate determination of actual atomic percentage compositions of each sample was done by a combination of the aforementioned density and lattice parameter values found for each sample. These values were used in the well known relationship (Ref 30:3-12):

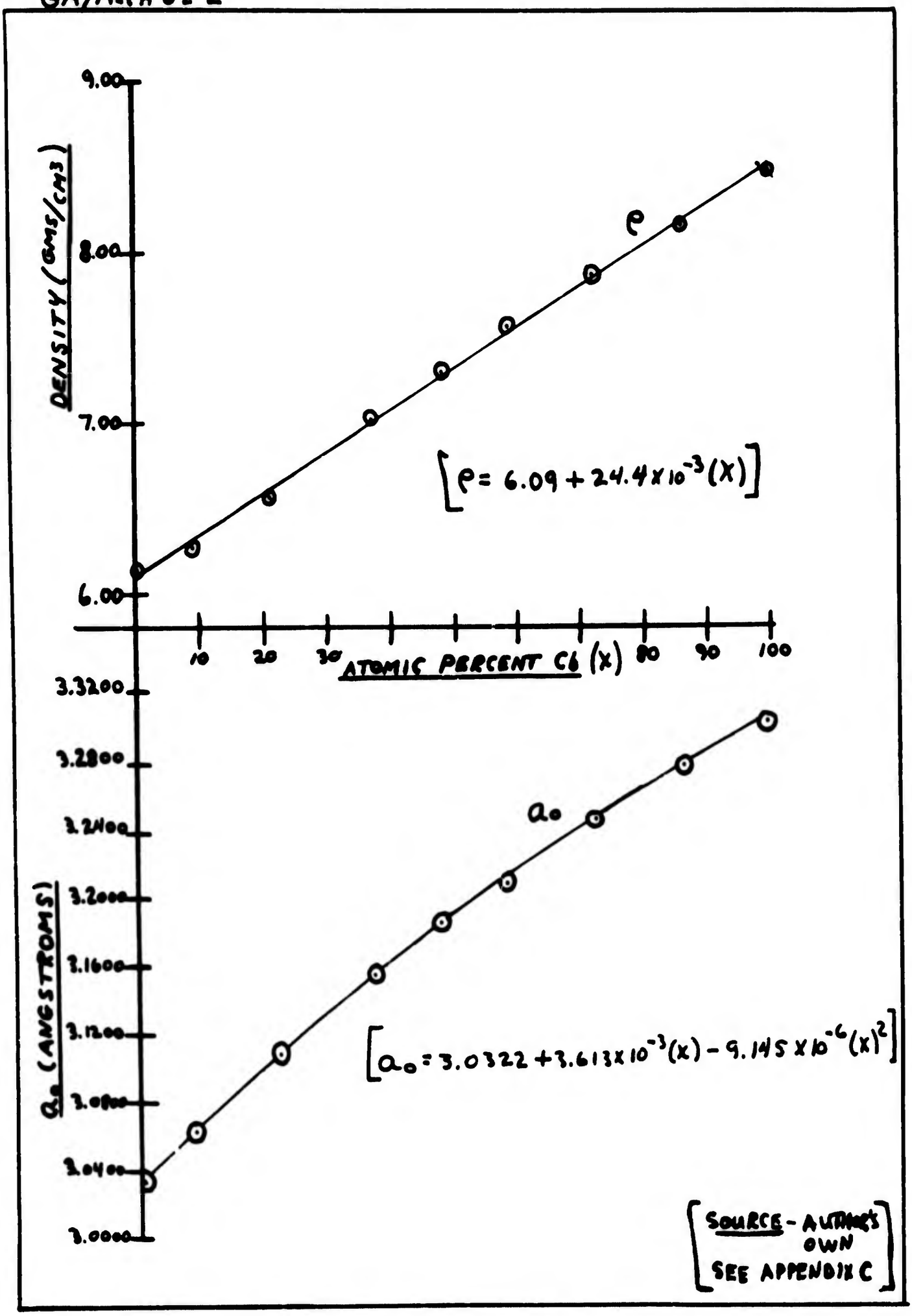

Figure 5- Variation of density and lattice parameter with atomic percent of Cb.

$$\text{Density} = \frac{(\text{No. atoms/unit cell})\ (\text{Atomic weight})}{(\text{Volume of unit cell})}$$

or, for this particular binary combination of vanadium and columbium:

$$\rho\ (\text{of alloy}) = \frac{2\left[x(92.91) + (1-x)\ (50.95)\right]}{A\ (a_o)^3} \quad (21)$$

where ρ is the density of the alloy in gms/cm , x is the atom fraction of columbium, A is Avogadro's number (and is 6.023×10^{23} atoms/gram-atom), 92.91 and 50.95 are the respective atomic weights of columbium and vanadium in grams/gram-atom, and a_o is the measured lattice parameter in centimeters. Rearrangement and algebraic manipulation yields:

$$x_{Cb} = \rho\,(a_o)^3\,(0.00717) - 1.214 \quad (22)$$

where a_o is now in angstrom units (10^{-8}cms).

Procedures used in measuring lattice parameters and density are described briefly in this section and in considerable detail in Appendix C. Results are shown in Figure 5 and are tabulated in Table II. The results are considered accurate to $\pm$ 1 a/o and variations up to 4 a/o from nominal compositions can be noted. Two reasons for this difference present themselves. The first is that the weight loss noted during the standards melt was almost all columbium, a not unreasonable assumption when the fact that the columbium consisted

TABLE II

VARIATION OF PROPERTIES OF Cb-V SOLID SOLUTIONS AS A FUNCTION OF COMPOSITION

SPECIMEN NUMBER	NOMINAL COMPOSITION (a/o C_b)	ACTUAL COMPOSITION (a/o C_b)	LATTICE PARAMETER (angstroms)	DENSITY (gms/cc)	MOLAL VOLUME (cc/mol)	PARTIAL VOLUMES J_{Cb}	MOLAL (cc/mol) V_v
1	0	0	3.0319	6.11	8.4	11.3	8.4
2	10	8	3.0612	6.25	8.8	11.3	8.3
3	25	21	3.1107	6.56	9.1	11.2	8.4
4	40	37	3.1541	7.01	9.2	10.5	8.6
5	50	48	3.1815	7.29	9.8	10.8	8.8
6	60	58	3.2092	7.55	10.0	10.9	8.6
7	75	72	3.2448	7.85	10.3	11.1	8.5
8	90	86	3.2775	8.16	10.6	11.2	7.8
9	100	100	3.3023	8.52	11.2	11.2	8.4

Source of lattice parameter and density data is author's own. (See Appendix C).
Partial molal volume calculations done after Klotz (Ref 17:13).

of tightly packed turnings is considered. The second reason is that the small weight percentage of the impurities can yield almost a full 2 a/o effect due to the low atomic numbers of the lighter elements. Partial molal volume data were also calculated from the derived data based on a method outlined in Klotz (Ref 17:13). The partial molal volume can be used to correct diffusion data for volume changes after the method of Baluffi (Ref 1:872-873) mentioned in Section II of this paper.

X-ray specimens for lattice parameter measurements were prepared by first filing each standard and saving the filings after a magnet had been passed through the powder to pick up any stray contamination from the steel file. Each powder specimen was then individually wrapped in tantalum foil and all were annealed at 1200°C. for 4 hours under a dynamic vacuum of 0.05 microns in the NIC vacuum furnace (Appendix B). Each powder filing was then individually mounted on cellophane tape for use as targets in the x-ray camera.

A Norelco 60-mm symmetrical focussing back-reflection x-ray camera was used for all precision lattice parameter measurements. Because the symmetric back-reflection camera employs diffraction angles(θ) near 180°, it was chosen for its optimum accuracy in parameter

determination. A copper target x-ray tube with a nickel radiation filter was used in all exposures. Power settings and specific data are summarized in Appendix C. Most of the diffraction lines for the specimens were sharp and distinct, indicating good work-relieving anneal. Since the fractional errors produced in this method are very closely proportional to $\phi \tan \phi$ (where $\phi = \pi/2 - \theta$) (Ref 9:11), this function was used in a linear extrapolation of each set of lattice parameters to $\phi = 0$ to determine a_o.

Only one other source of x-ray data on the columbium-vanadium binary system has been found in the literature. Wilhelm, et al (Ref 31:917), published a set of lattice parameter variations with composition for this system. However, his values for lattice parameters in the columbium end of the solid solutions were, in Pearson's words "... incredible ..." (Ref 22). The x-ray findings of this paper confirmed Pearson's succinct evaluation of Wilhelm's reported values.

After the atomic percentages of each alloy were calculated, the standard alloys were shipped to Advanced Metals Research Corporation, Somerville 45, Massachusetts, to be used as standards for subsequent electron probe analysis of diffusion zones. Diffusion

zone electron probe analysis was done for this thesis under Air Force contract by Advanced Metals Research Corporation. Informal telephone conversation with Advanced Metals Research Corporation personnel indicated that electron probe calibration with the submitted standards showed no microinhomogeneities in the standard specimens.

Diffusion Couple Preparation

Diffusion couple preparation was done concurrently with alloy standards preparation. It was decided to have diffusion couple elements of columbium (hereafter abbreviated as Cb), vanadium (V), and a 50 a/o Cb intermediate alloy. Columbium rod was on hand from the original columbium ingot that was turned down to provide turnings for the alloy standards. The original ingot was turned down to about $\frac{1}{2}$-inch diameter and then swaged to a $\frac{1}{4}$-inch diameter rod. Vanadium chips and a combination of chips and columbium turnings were compacted to form approximately 150 gram specimens of the pure vanadium and of the 50:50 a/o Cb-V alloy. These were arc-melted at the University of Dayton using the same procedure described in the previous discussion. The rectangular ingots thus formed were then turned down to $\frac{1}{2}$-inch diameter. Each of the two $\frac{1}{2}$-inch diameter bars was then coated with a chromic oxide

GA/MECH 62-2

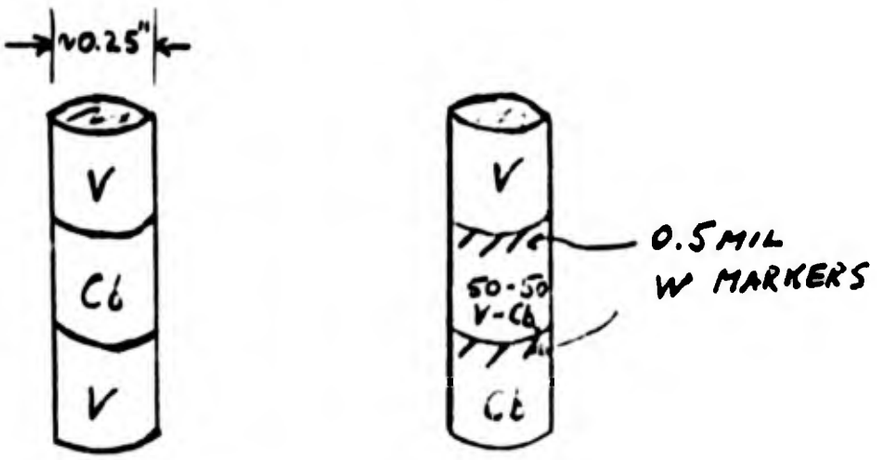

A. DIFFUSION COUPLE MAKEUP.

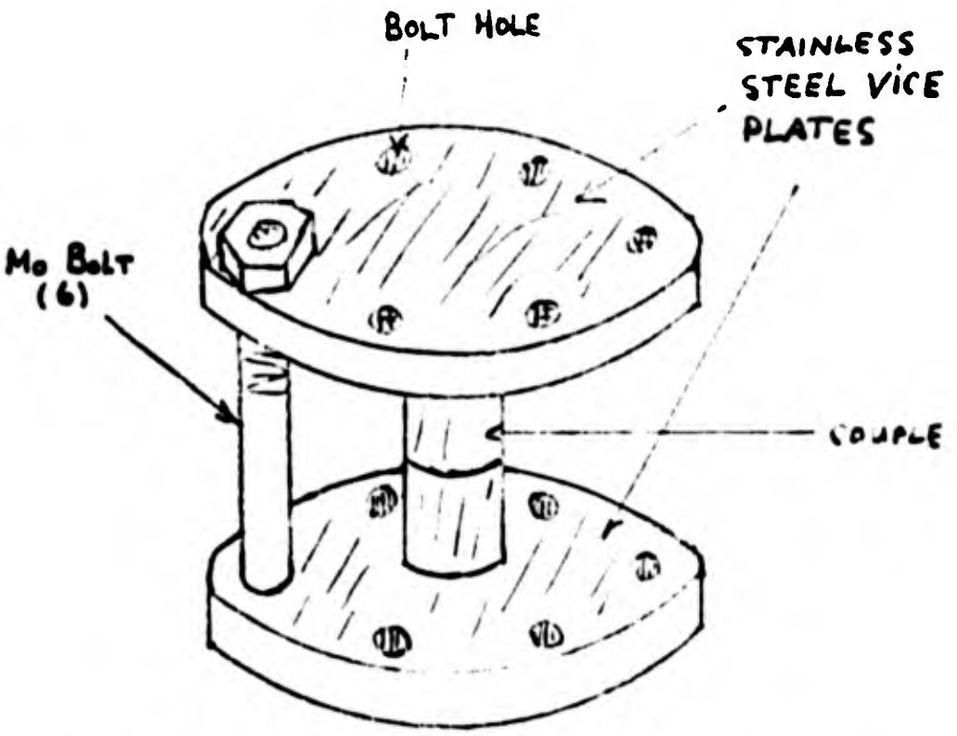

B- DIFFUSION COUPLE ASSEMBLED IN BONDING VICE.

Figure 6- Diffusion couple make-up and bonding technique.

slurry parting compound and tightly fitted into ½-inch stainless steel tubing "cans". The cans were evacuated, sealed, and then swaged to about 3/8-inch outside diameter at 1100°C. at Battelle Memorial Institute, Columbus, Ohio. Both bars and the columbium rod were then annealed at 1300°C. for 16 hours under a dynamic vacuum of 0.04 microns to complete homogenization.

After final homogenization anneal, the vanadium and the 50:50 a/o Cb-V alloy bars were machined to ¼-inch diameter rod. Then all three rods, including the columbium rod were cut into ¼-inch long cylinders with plane and parallel ends. The cylinders were mounted in metallographic mounts and their ends polished down to 400 grit paper. Each diffusion couple was individually built up in a stainless steel vice as shown in Figure 6. When each couple was assembled in the vice, the top of the vice was carefully lowered and the molybdenum holding bolts were tightened with pliers. A bonding anneal of 3 hours at 1000°C. at 0.05 microns vacuum completed the couple.

Four diffusion anneals were planned for this paper, therefore four pairs of diffusion couples were made. One couple of each pair was pure V-Cb-V with no Kirkendall markers. The experimenter tried vainly for

one week to realize a successful bond anneal with tungsten markers at the metal interfaces. No reason can be offered for the couples' failure to bond with the markers in place. The other couple assembly was V-50:50 a/o Cb-V alloy-Cb with 0.5 mil (0.0005 inch) diameter tungsten wire markers inserted between the metal interfaces. This couple type bonded satisfactorily with the markers in place (Figure 6). The above arrangement of combinations in the couples would result in four diffusion zones at each annealing temperature.

Diffusion Anneals

It was decided to perform the diffusion anneals as close to the melting point of the alloy as possible to reduce the elapsed time the anneal consistent with obtaining a diffusion zone wide enough for analysis. It has been shown that the total width of the diffusion zones is approximately equal to $8\sqrt{D\,t}$ (Ref 25) for a given temperature (assuming D is constant over the concentration range) and this relation was used in determining approximate diffusion anneal times. D for the self diffusion of Cb was chosen as the most conservative diffusivity of the system being investigated and was the D used in the rough calculations (Ref 23:60-61).

For temperatures above 1500°C., ten days at temperature would provide a diffusion zone of ample width for electron probe analysis. As the lowest melting point of the columbium-vanadium system is 1825°C. (Ref 11:1022), it was decided to have diffusion runs at 1750°C., 1600°C., 1500°C., and 1400°C.

1750°C. Diffusion Anneal. The first diffusion anneal was performed in the ABAR vacuum furnace (Appendix B) at 1750°C. (± 10°C.) for 188.9 hours at a vacuum of 0.003 microns. However, the experimenter had neglected to check the vapor pressure of vanadium at 1750°C. (It is 4.25 microns (Ref 26)) and the pure vanadium portions of the couples almost completely evaporated in the furnace to condense on the cooler radiation shields. The columbium-50:50 a/o Cb-V alloy portion of one couple was salvaged for analysis, thus providing one good diffusion zone from the run.

1400°C. Diffusion Anneal. The second diffusion anneal was performed in the NRC vacuum furnace (Appendix B) for 400.85 hours at 1403°C. (± 21°C.). The vapor pressure of vanadium at 1400°C. was carefully checked (0.005 microns) against the known vacuum of the NRC furnace (0.01 microns). The couples were wrapped in tantalum foil, weighed to the nearest ten-thousandth of a gram, and then

suspended in the furnace hot zone in a molybdenum bucket. Temperature was regulated manually through a Powerstat control and was continually monitored by a recorder registering the output of a platinum-platinum 10% rhodium thermocouple. Four shutdowns and reheat cycles were programmed into the diffusion run (including initial heating and final shutdown) to check on thermocouple condition and weigh the specimens for any sensible weight loss. There was no apparent vanadium loss throughout the entire run. Heating time from room temperature to diffusion anneal temperature was less than six minutes in all cases. Cool down time from diffusion anneal temperature to below 800°C. was less than three minutes in all cases. Since the total time at annealing temperature was in excess of 400 hours and the combined reheat and cooling down cycles did not exceed 0.63 hours, the heating and cooling times for this run were considered instantaneous in this paper.

1600°C. Diffusion Anneal. The 1600°C. diffusion anneal was beset with technical and experimental difficulties. Because of the aforementioned vapor pressure of vanadium, it was planned to perform the diffusion anneal in the Marshall furnace under purified helium at one

atmosphere pressure (Appendix B). Three separate attempts at a diffusion anneal in the Marshall furnace met with furnace liner failure with resultant equipment destruction and time loss. The general scheme was to have the specimens mounted on a long tantalumrod and, after the furnace reached temperature, insert the specimens into the hot zone from the cool part of the furnace, and retract them after the requisite amount of time elapsed at temperature.

The first attempt at 1600°C. was made with no provisions to protect the mullite furnace liner from thermal shock as the cold specimen was entered into the hot zone. Also, heavy brass fitting plugs at the end of the glass extension of the mullite tube were used to permit gas line inlets, wire outlets, and positioning rod access. The mullite tube cracked and disintegrated after 6.25 hours at temperature. The helium atmosphere prevented diffusion couple spoilage and the specimens were retracted out of the hot zone to cool before the furnace cooled down to permit repairs.

The second attempt met with complete furnace liner failure during heat-up. After this failure, it was decided to discard the heavy brass plugs and have glass fitted plugs manufactured to prevent

detrimental static bending loads on the liner at temperature and also preclude glass end cracking due to excessive thermal expansion of the plugs.

The third attempt, using the glass plugs and a second smaller diameter mullite tube inside the main furnace liner in the hot zone to prevent thermal shock failure, was also unsuccessful and netted not only complete failure of the mullite liner, but complete deterioration of the diffusion couples. This failure was not noted until the run was considered complete after 204 hours at temperature and the furnace was being dismantled so it could be unloaded.

Further attempts to use the Marshall furnace for a 1600°C. anneal were abandoned after the third failure.

With time and equipment becoming of prime importance, the experimenter resolved on an expedient to enable the relatively reliable vacuum furnaces to be used for the 1600°C. diffusion anneal. Two 3-inch long, $\frac{1}{2}$-inch diameter solid molybdenum bars were reamed out to 7/16-inch inner diameter. The cylinders and two diffusion couples were taken to Battelle Memorial Institute where the diffusion couples were placed in the cylinders and molybdenum caps welded on to encapsulate the couples. The entire operation

was done in an inert helium atmosphere so that the couples were sealed in molybdenum under one atmosphere of helium. This treatment, it was felt, made the two diffusion couples impervious to all but the most extreme experimental mishaps.

The fourth, and finally successful, attempt at a 1600°C. anneal was made with the molybdenum-encased couples in the NRC vacuum furnace using a manual temperature control through Powerstat settings with a tungsten-tungsten 26% rhenium thermocouple as temperature indicator. Total anneal time was 190 hours at a temperature of 1620°C. (± 20°C.).

1500°C. Diffusion Anneal. The 1500°C. diffusion anneal followed the pattern of the successful 1600°C. anneal attempt discussed above. Because of the specimen destruction in the unsuccessful runs in the 1600°C. anneals, material for only one couple remained for the 1500°C. run. This couple consisted of Cb-50:50 a/o Cb-V alloy-V elements with 0.5 mil diameter tungsten markers. As the 1600°C. run, the couple was sealed in a solid molybdenum cylinder and welded shut in a helium atmosphere.

The 1500°C. diffusion anneal was made with the molybdenum encased couple in the NRC vacuum furnace using a manual temperature control through a Powerstat with

a tungsten-tungsten 26% rhenium thermocouple temperature readout. Total anneal time was 176 hours at a temperature of 1505°C. (± 20°C.). The run was scheduled for 300 hours at temperature, but furnace failure terminated the run at 176 hours.

BLANK PAGE

IV. Experimental Results

The results of the microbeam probe analysis are plotted as a series of concentration gradients in Figures 7 through 12. The results of the computer program on the resultant data are presented in graphical form in Figures 13 through 16. The computer program used in the Matano solution of the concentration-penetration curves using the data from the microbeam probe analysis of the diffusion zones of the diffusion couples is outlined in Appendix D. Also, the raw input data from the microbeam probe analysis are tabulated in this Appendix (Table VI).

Two parallel sets of results are presented. First, the information as it is normally presented with the diffusivities and frequency factors in cm^2/hour, and second, the same information presented with the distances converted to atomic lattice parameters (lp) and the diffusivities and frequency factors presented in lp^2/hour (Figures 13 through 16 and Table III). The change in distance units corrects the data for molal volume changes as outlined in Section II. The conversion of penetration data was done by dividing the distance increments by the appropriate concentration value of lattice parameters from Equation C-3 (Appendix C). Values of activation

energies are also tabulated for both sets of results in Table III.

The plethora of data available from the computer program makes tabulation of anything but results impractical. Data available from the computer program is summarized in literature (Ref 12). For this thesis, in every case where the diffusivities are presented as a function of concentration, at least one calculation was done manually to check the general validity of the results. Only relatively minor differences for a value of D and a given data point were noted between the computer values and manual values.

Excellent agreement is seen in comparing the derived diffusivities and activation energies at high Cb and V concentrations from this thesis with the diffusivities and activation energies for Cb and V in similar substitutional diffusion (Ref 23:60-61, 108).

An experimental error can be noted in the 1505°C. anneal results. Apparently the author inadvertently made a V-50-50 a/o Alloy-V couple instead of the V-50-50 a/o Alloy-Cb couple desired.

A minor disappointment was experienced in that only one set of Kirkendall markers were found during

electron probe analysis of the diffusion zones (1404°C. anneal). Time considerations prevented further metallographic search of the specimens by the author as the specimens had not been returned at the time of this writing. Simultaneous solutions of (13) and (15) show that for a concentration of 12.7 a/o Cb at 1404°C.:

$D_V = 6.6 \times 10^{-4}$ cm²/hour, $D_{Cb} = 3.8 \times 10^{-4}$ cm²/hour or D_V is about 1.73 times as great as D_{Cb}.

Tabular values of frequency factors and activation energies presented in Table III were conventionally derived from the best least squares straight line through the values of ln D versus 1/T. The frequency factor (D_o) is then the intercept at T = ∞, and the activation energy (Q) is derived from the slope of the straight line multiplied by the gas constant (R = 1.9859 calories/ mole °K.) Each value presented in Table III was derived from a minimum of three data points. Figures 17 through 20 show plots of $\log_{10}$ D versus 1/T.

Table III

D_o and Q as a Function of Composition

Composition (a/o Cb)	D_o (cm^2/hr)	Q (kcal/mol)	Do (ip^2/hr)	Q (kcal/mol)
95	1.23	71.1	7.0×10^{15}	69.4
90	3.81	74.5		
85			1.0×10^{17}	77.8
75*	0.24	55.3		
70			4.1×10^{16}	65.4
65	1.27	59.5		
60			1.6×10^{16}	59.9
55	0.97	64.9	9.5×10^{14}	48.1
45			9.2×10^{15}	56.2
35			8.9×10^{15}	55.8
30*	0.10	47.1		
20	3.65	59.0		
10	2.6	57.6		
5	2.26	57.1	5.3×10^{16}	59.8

* Derived from questionable regions of diffusivity versus concentration data (Ref Figures 13 through 16).

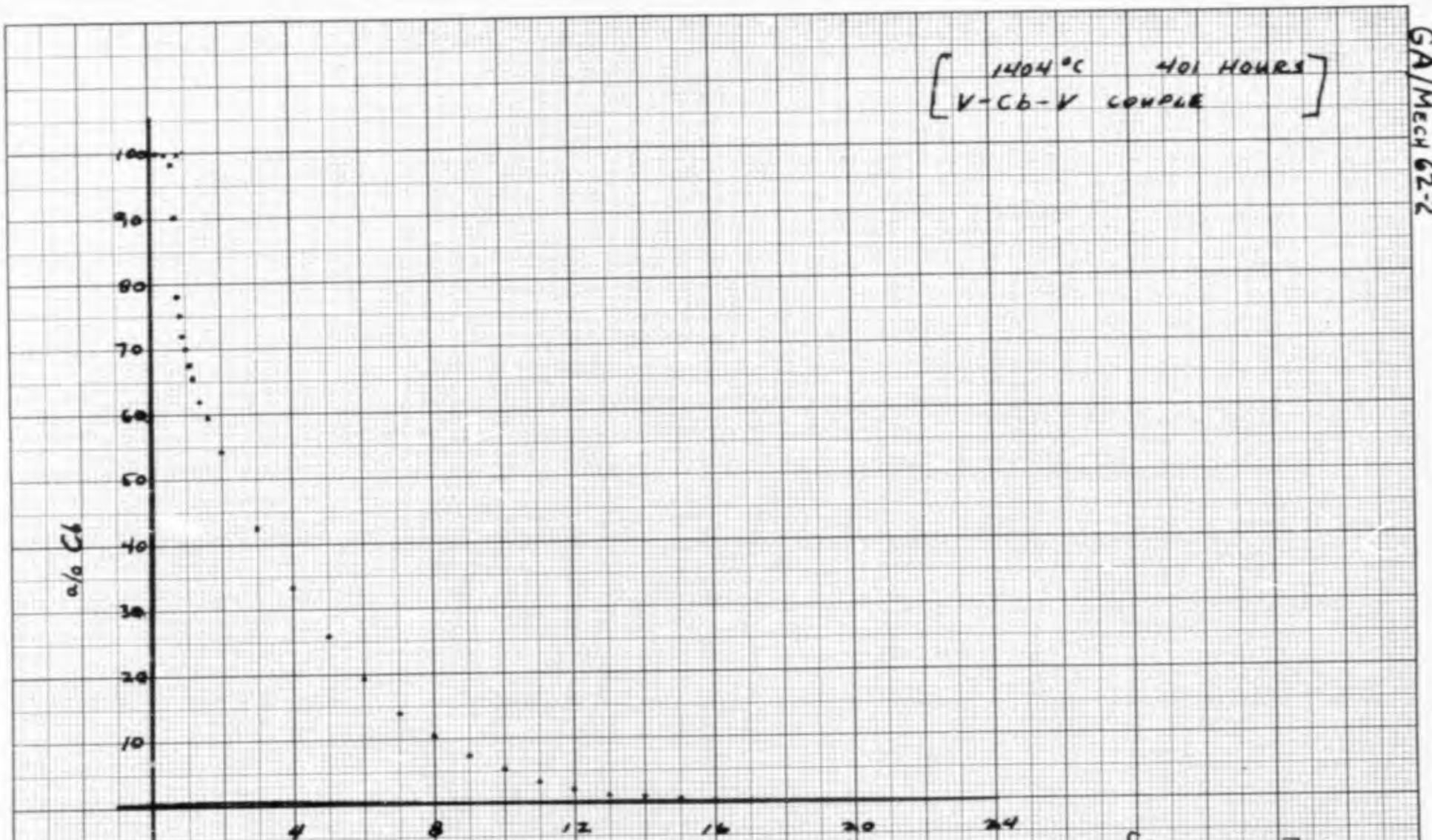

FIGURE 7 – CONCENTRATION GRADIENT 1404°C./401 HOURS – PURE METAL COUPLE.

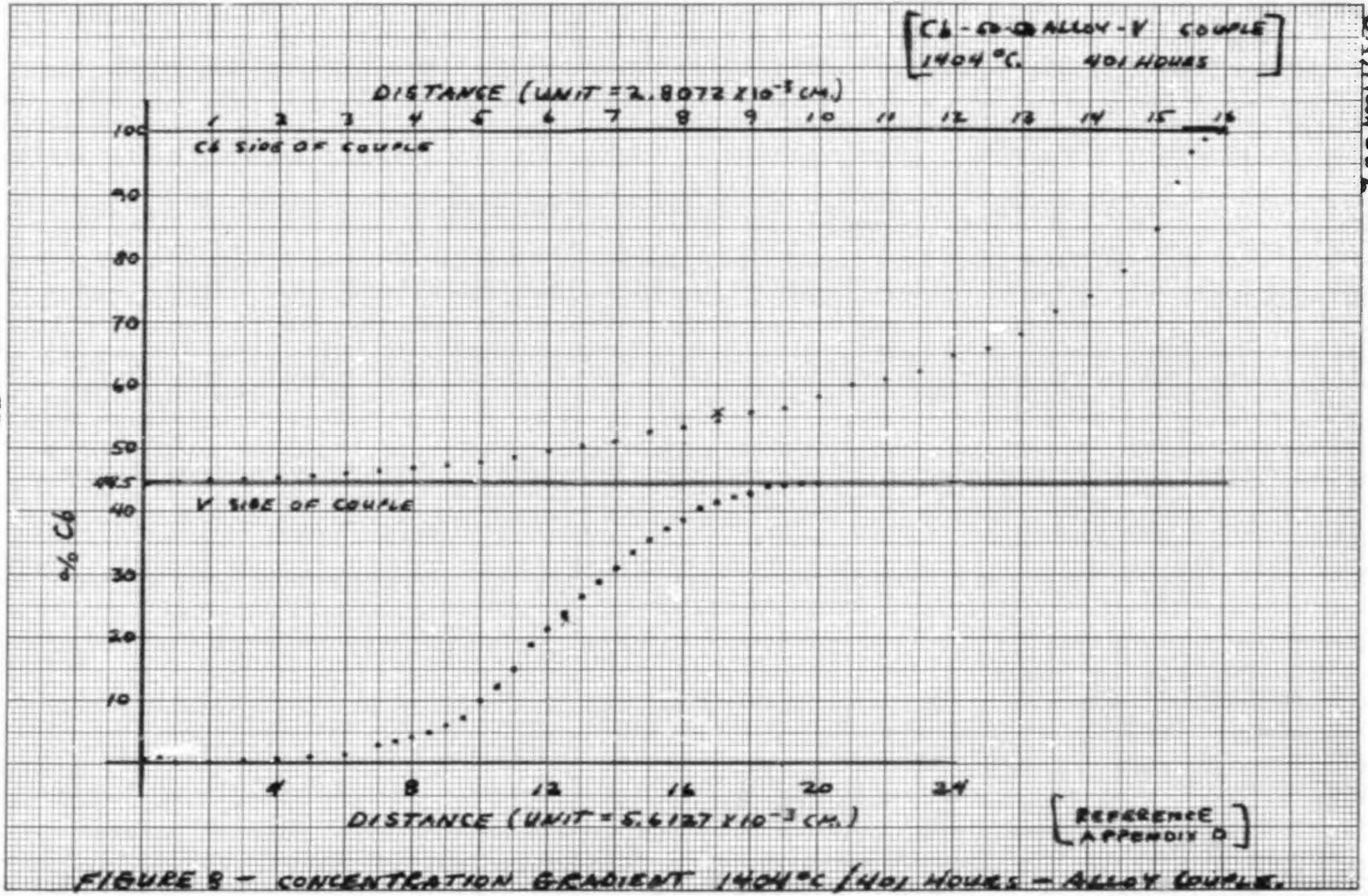

FIGURE 8 – CONCENTRATION GRADIENT 1404 °C / 401 HOURS – ALLOY COUPLE.

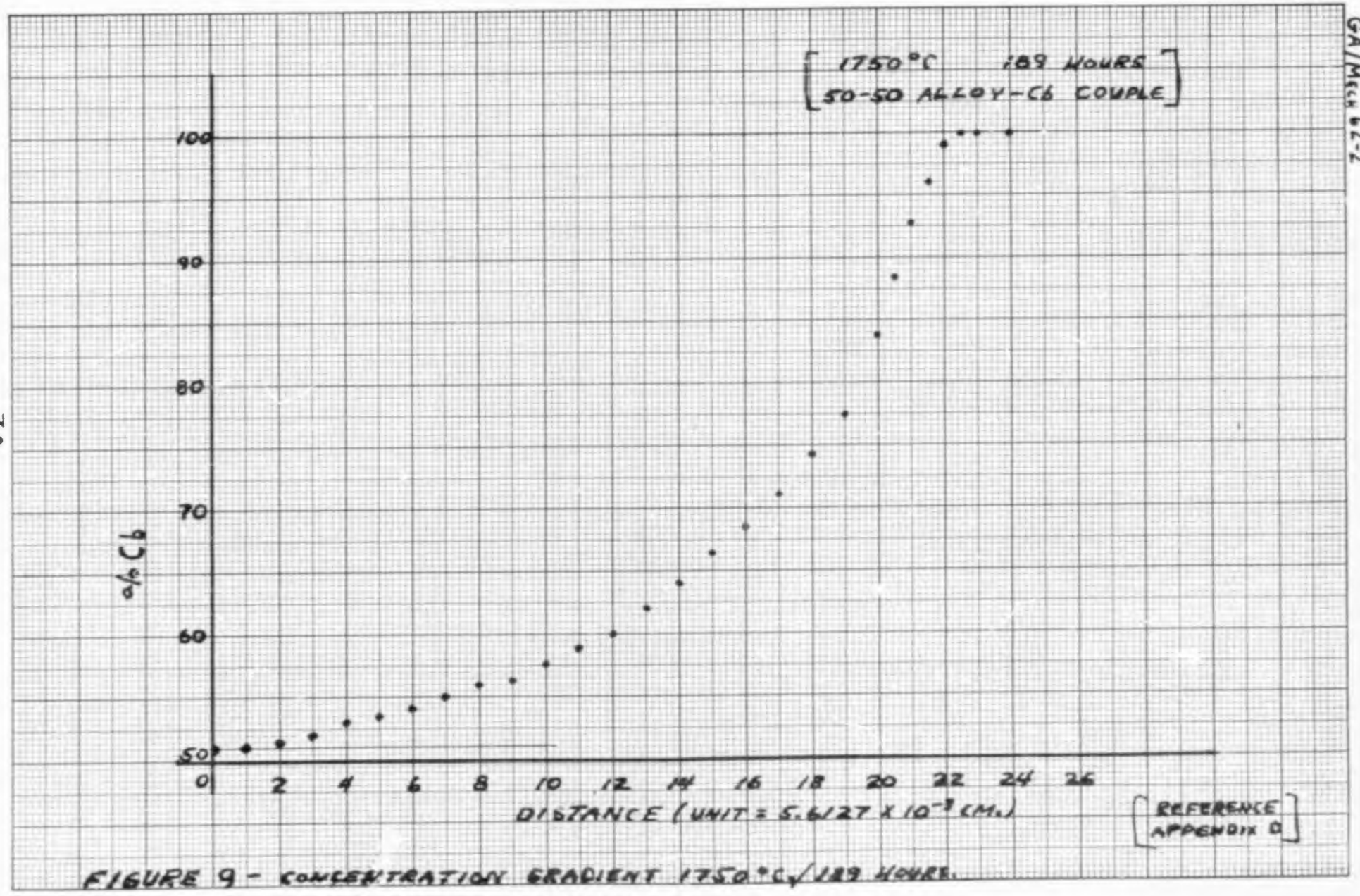

FIGURE 9 - CONCENTRATION GRADIENT 1750°C / 189 HOURS.

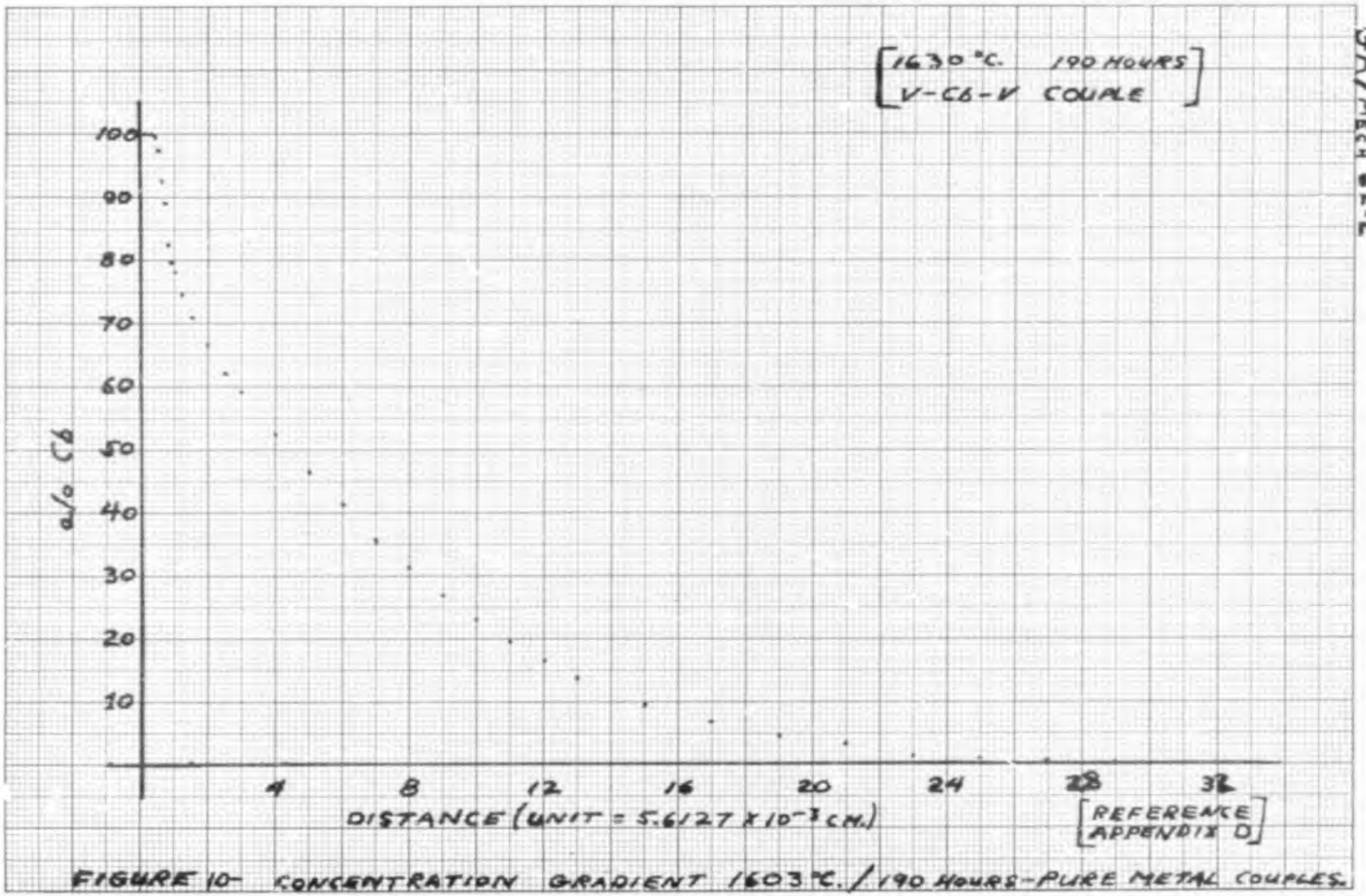

FIGURE 10- CONCENTRATION GRADIENT 1603 °C. / 190 HOURS - PURE METAL COUPLES.

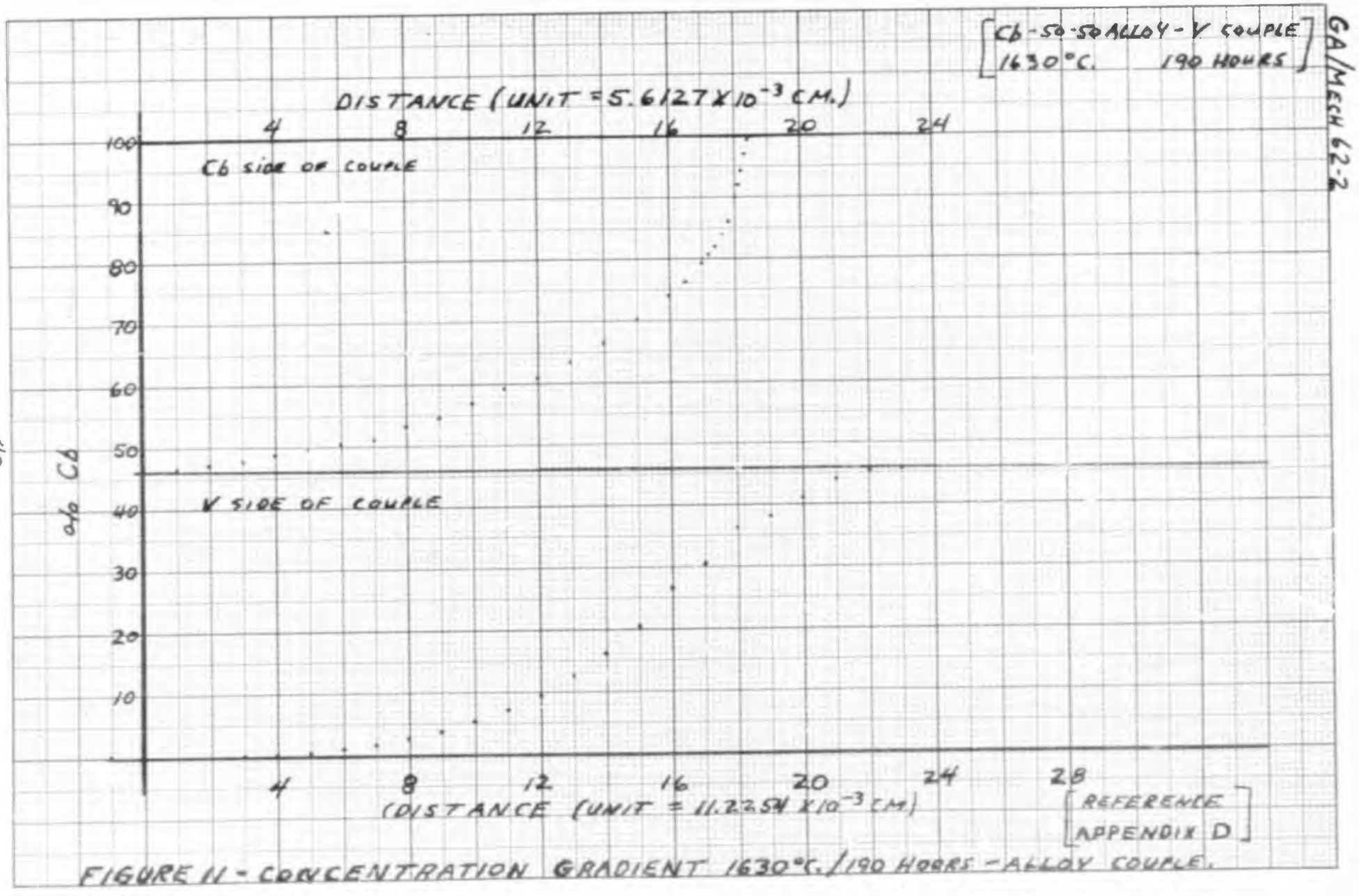

FIGURE 11 - CONCENTRATION GRADIENT 1630°C./190 HOURS - ALLOY COUPLE.

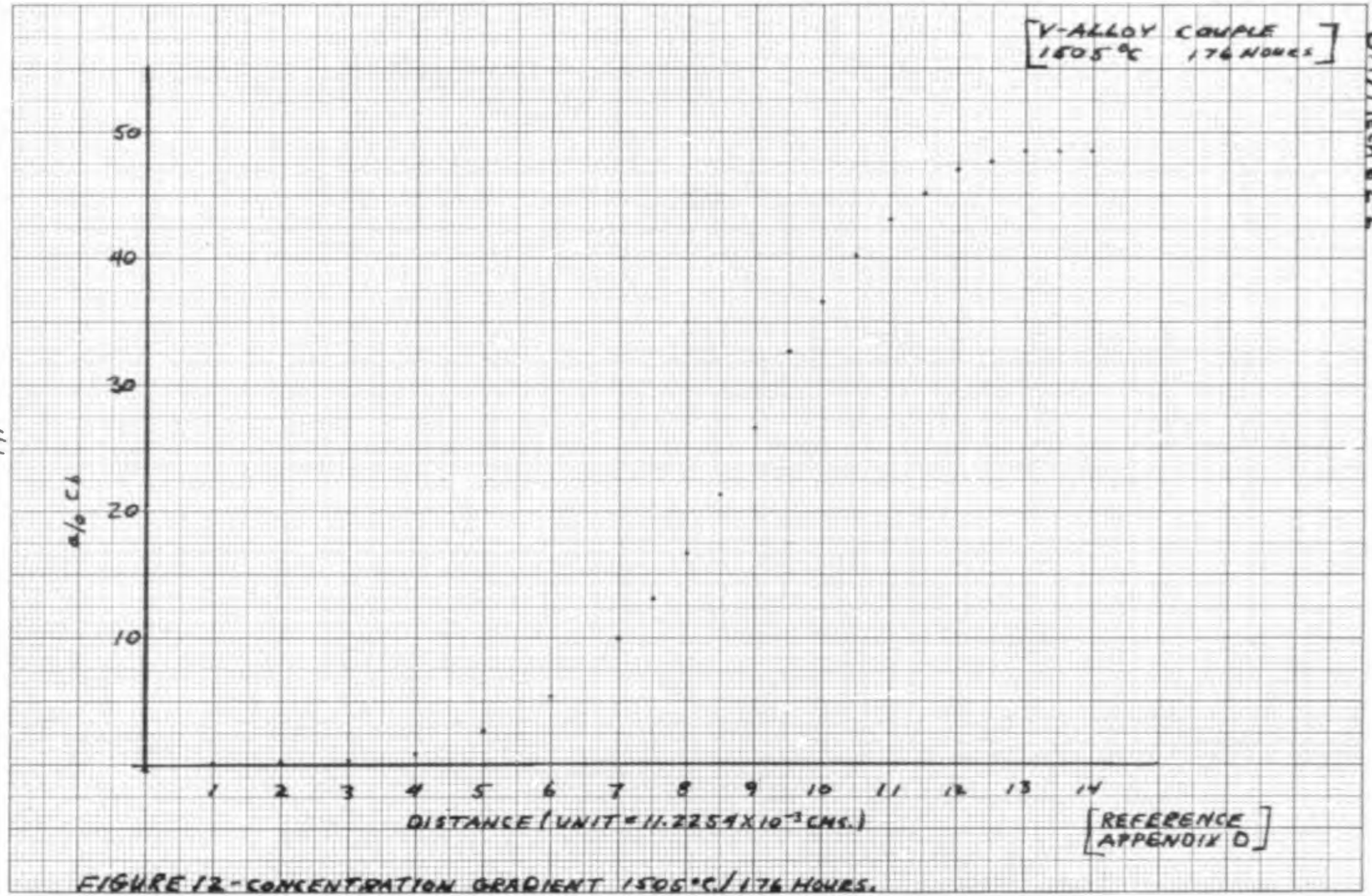

FIGURE 12 - CONCENTRATION GRADIENT 1505 °C / 176 HOURS.

GA/MECH 62-2

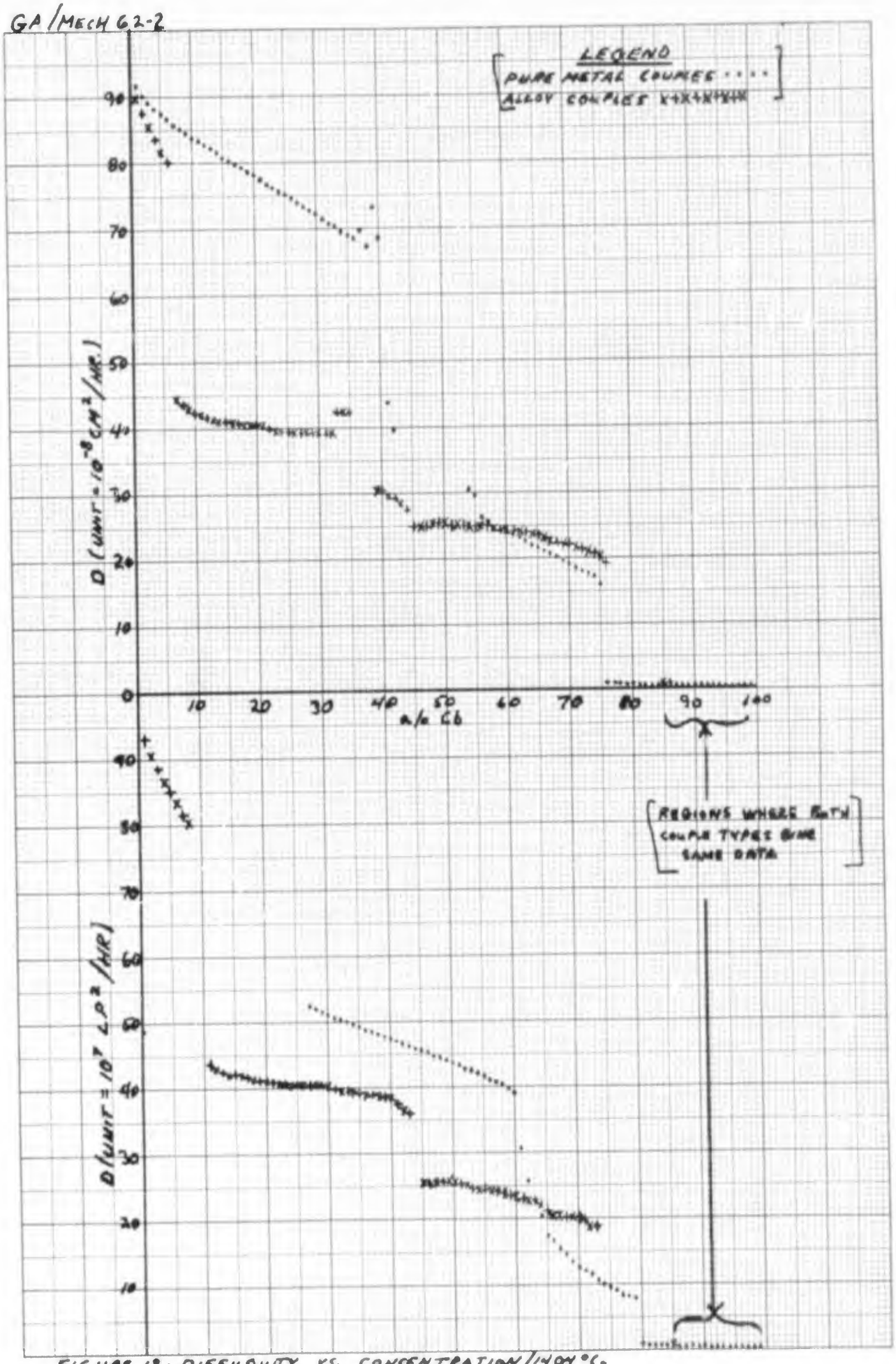

FIGURE 18 - DIFFUSIVITY VS. CONCENTRATION/1400°C.

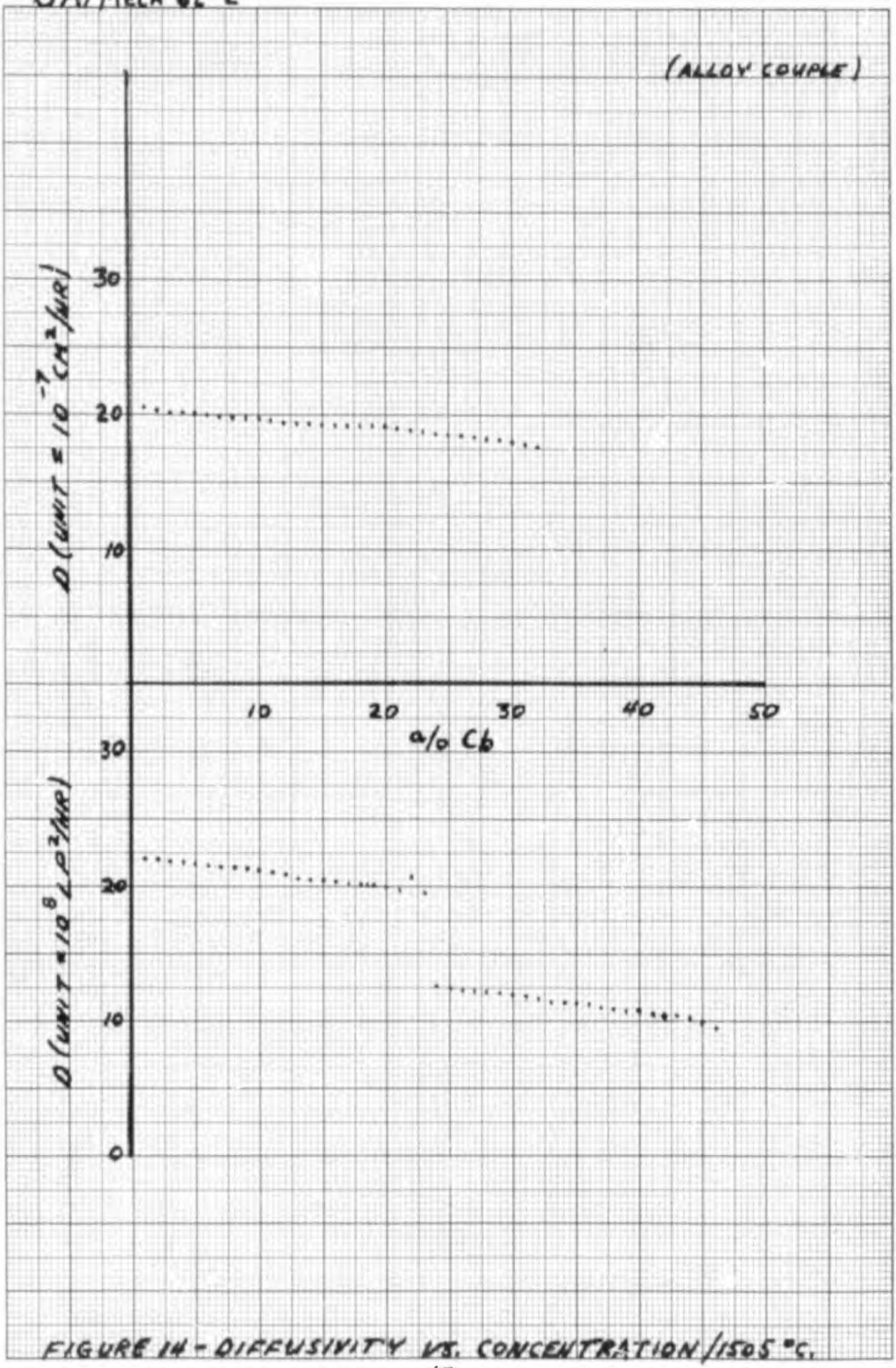

FIGURE 14 - DIFFUSIVITY VS. CONCENTRATION / 1505 °C.

GA/MECH 62-2

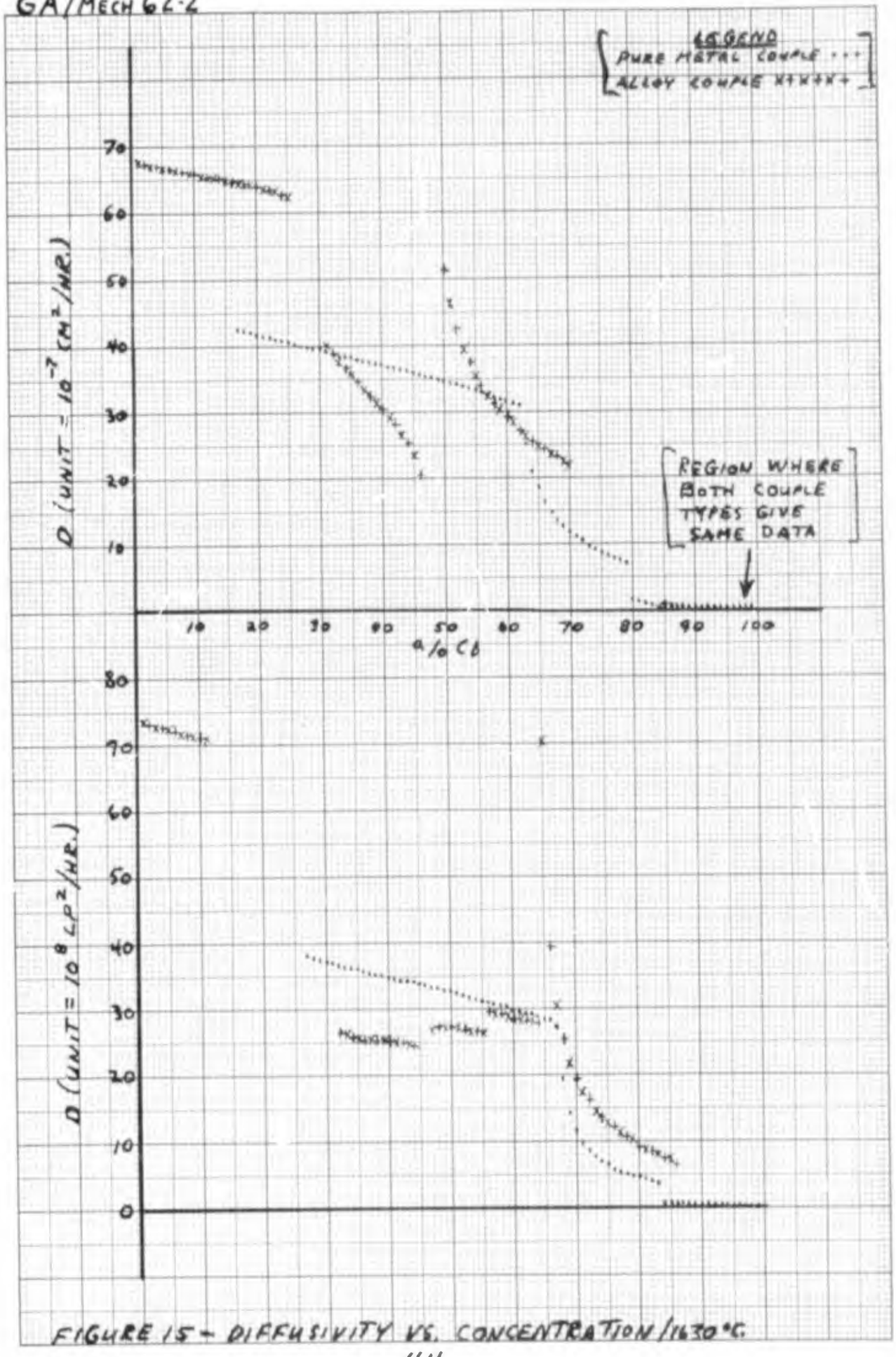

FIGURE 15 - DIFFUSIVITY VS. CONCENTRATION / 1630 °C.

GA/MECH 62-2

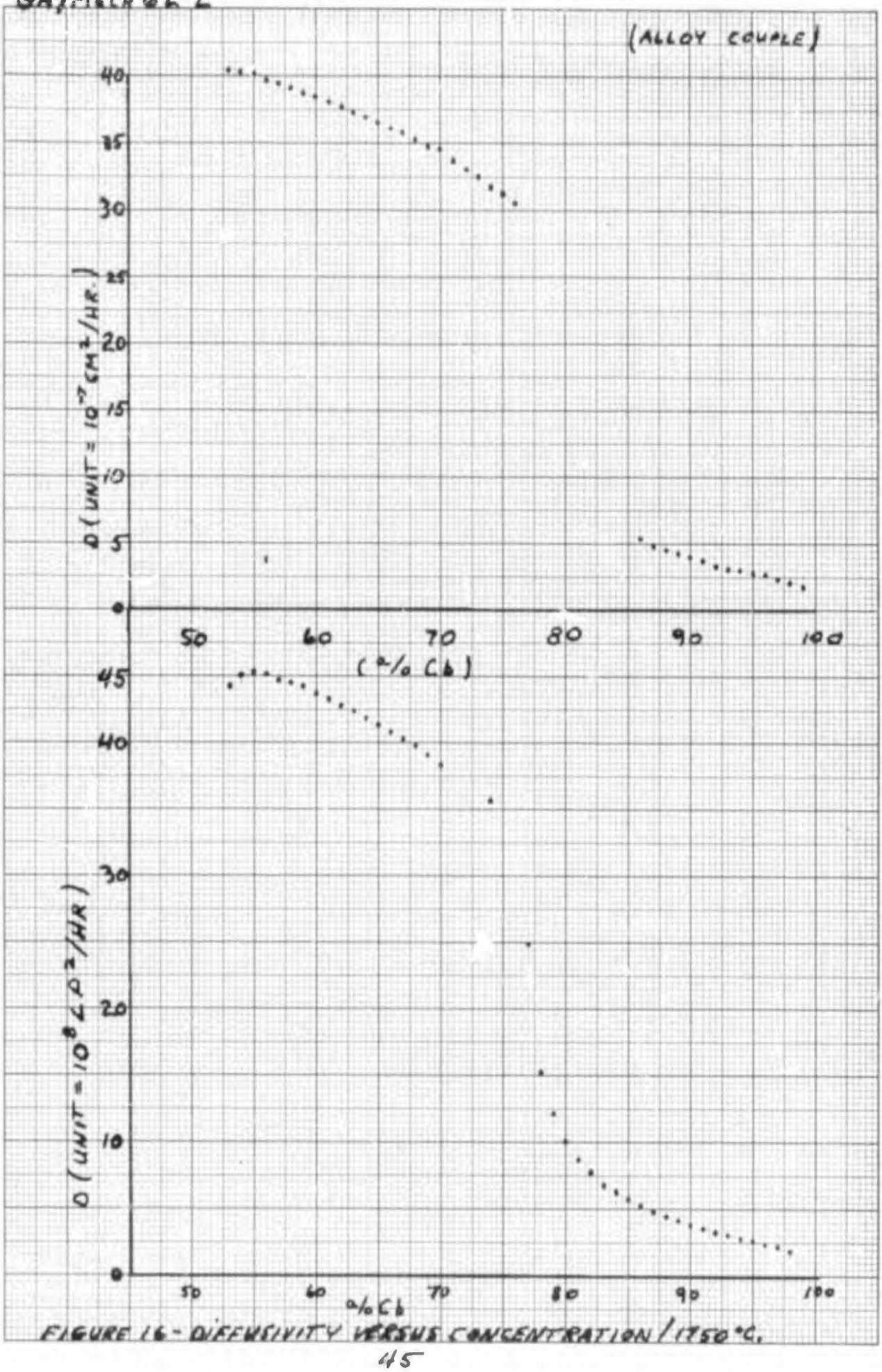

FIGURE 16 - DIFFUSIVITY VERSUS CONCENTRATION / 1750 °C.

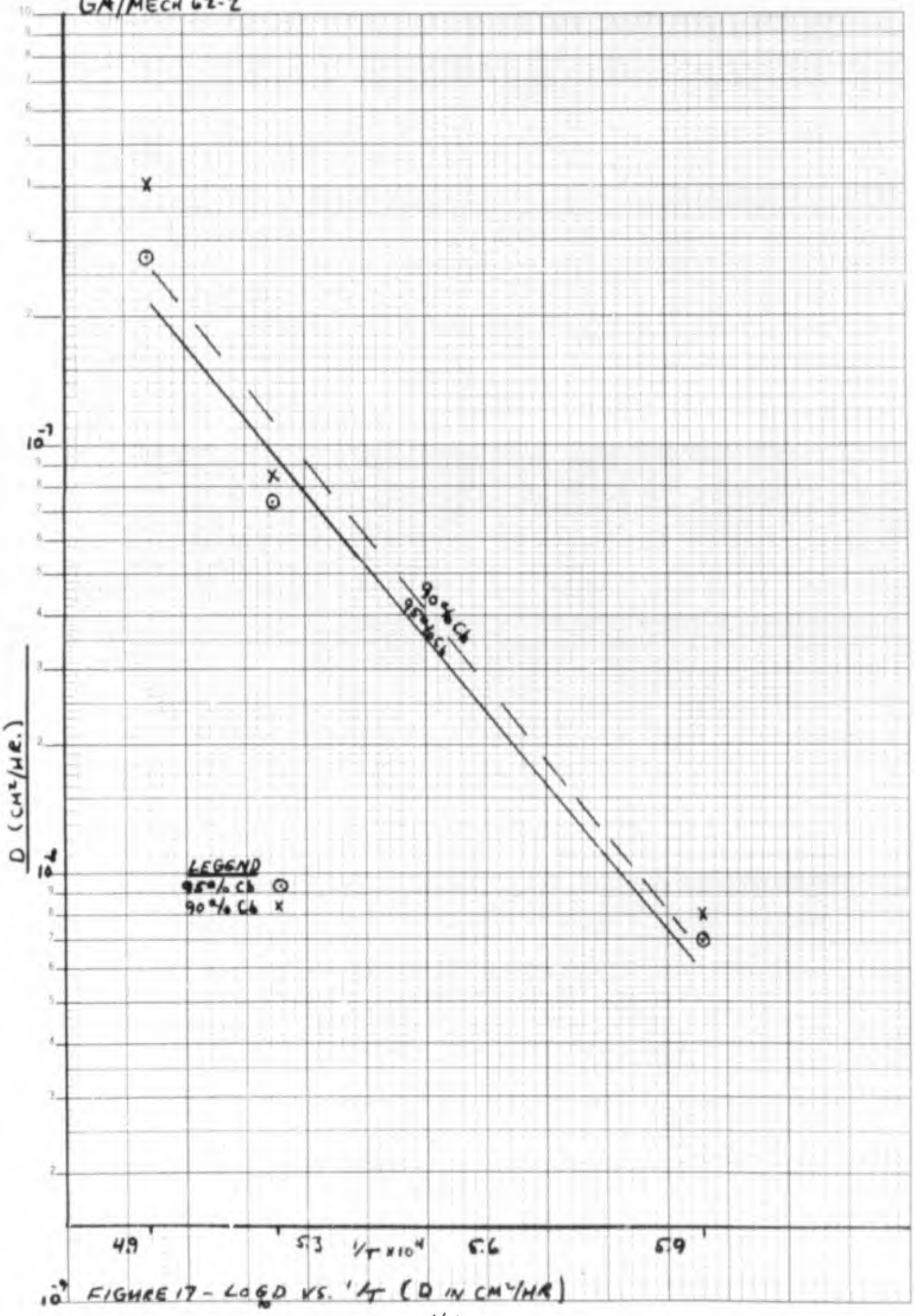

FIGURE 17 - LOG D VS. 1/T (D IN CM²/HR)

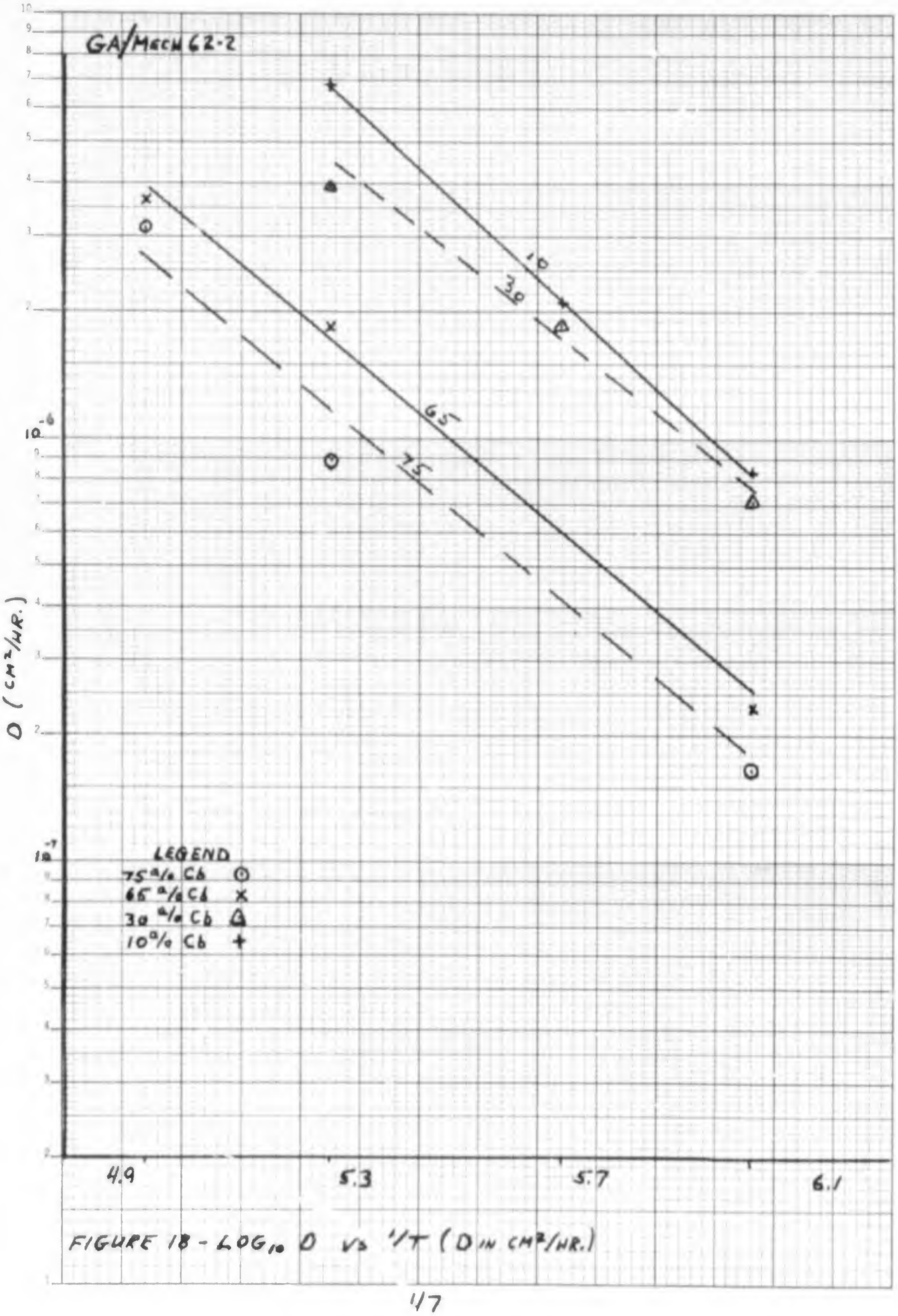

FIGURE 18 - LOG$_{10}$ D vs 1/T (D IN CM²/HR.)

GA/MECH 62-2

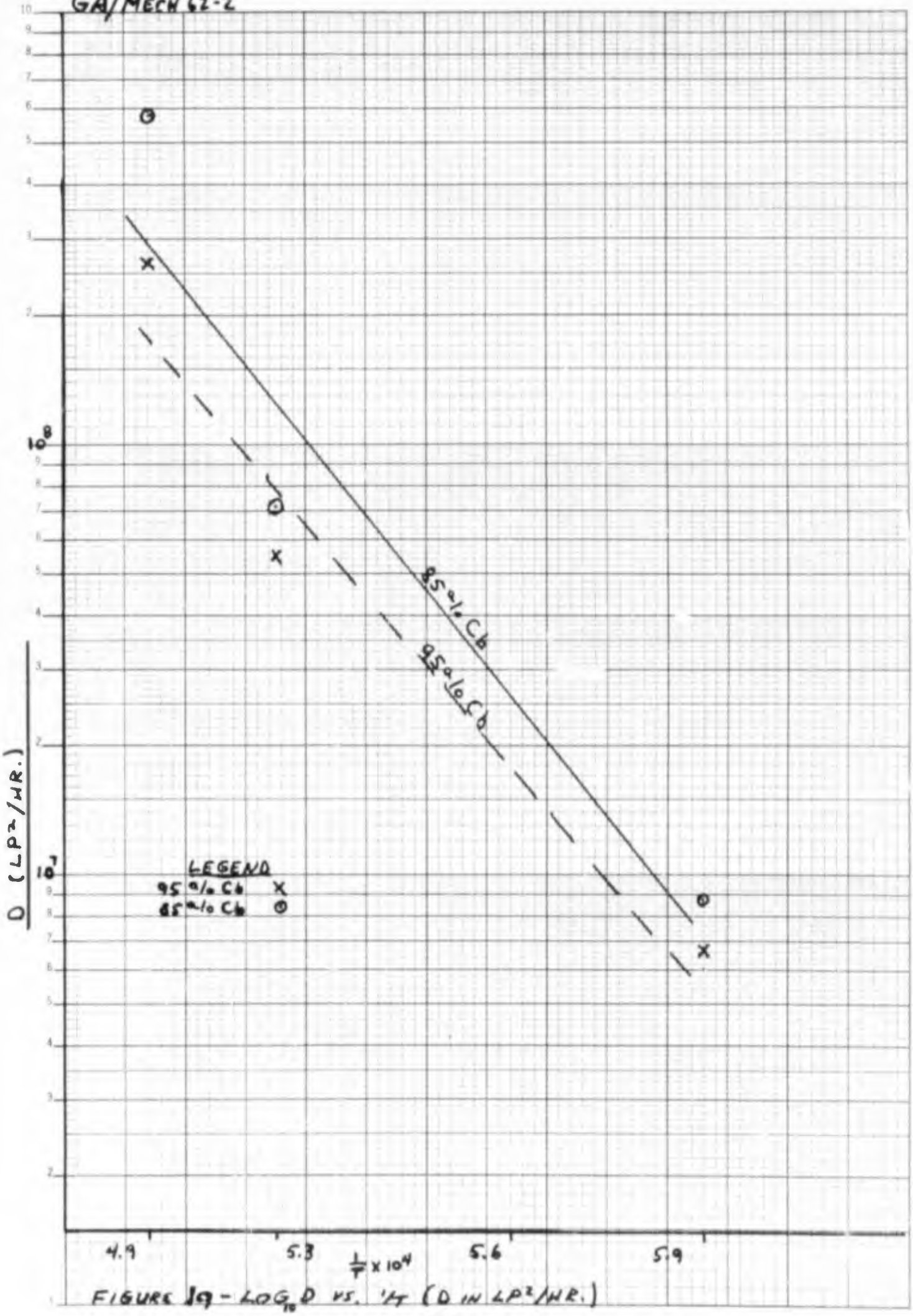

FIGURE 19 - LOG_{10} D VS. 1/T (D IN LP²/HR.)

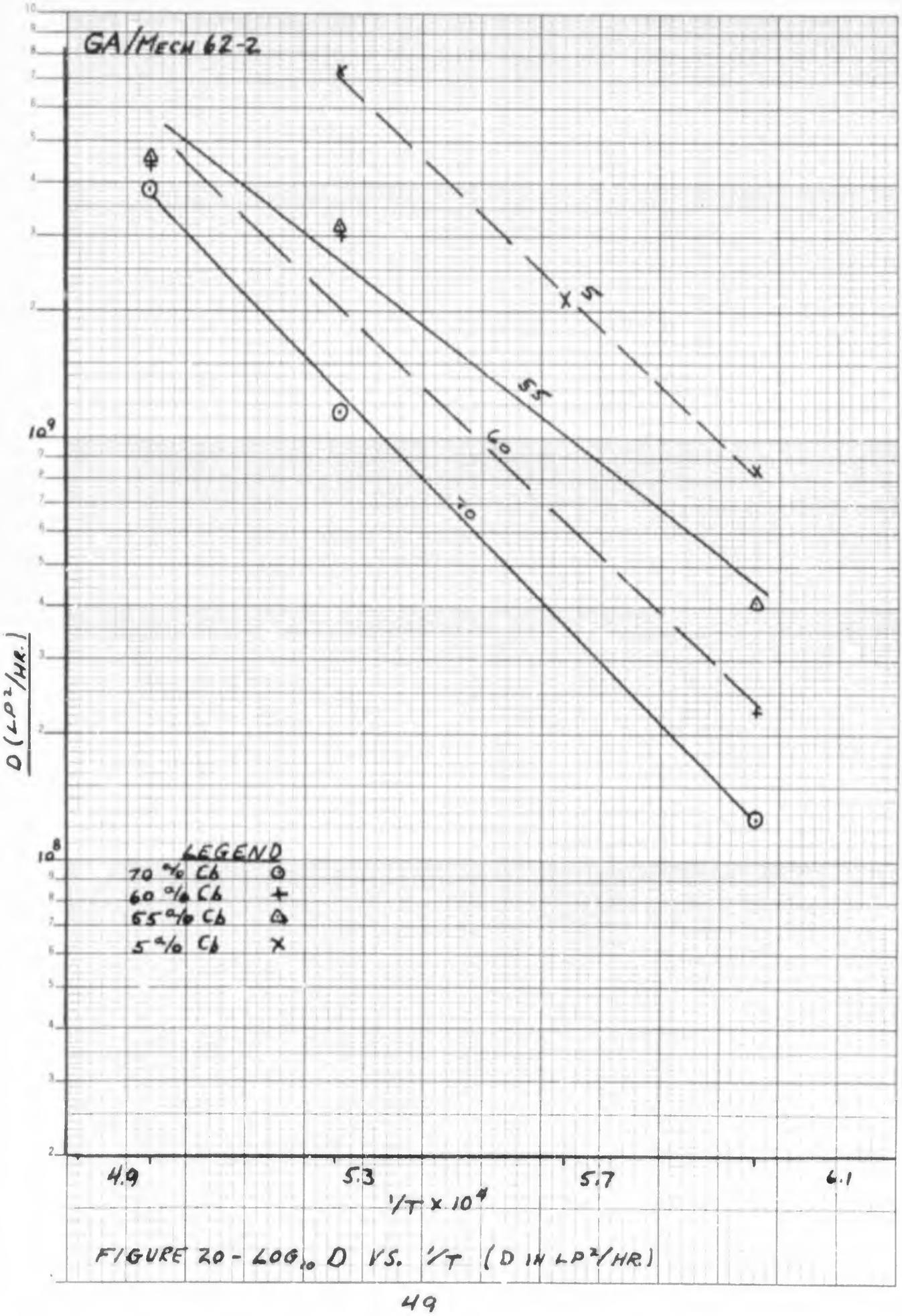

FIGURE 20 - LOG_{10} D VS. 1/T (D IN LP²/HR.)

V. Conclusions and Recommendations

General

The combination of two precision techniques, the microprobe analysis of the diffusion zones and the computer program for calculating diffusivities by the Matano method, represents a giant step forward, if not a breakthrough, in accurate diffusion studies. Although not the ultimate panacea for the Matano analysis of diffusion data, the computer technique described in Appendix D does relieve the experimenter of long laborious manual calculations and uncertain slope measurements in finding diffusivities. Additionally, he is practically assured that the only error resulting in this particular analysis, other than inherited from experimental procedure, will be the accuracy of the curve fit he directs the computer to use on the concentration data. Similarly, electron microprobe analysis of narrow diffusion zones reduces the error inherent in these analyses by a factor of 10 over former precision measurements of diffusion zones taken perpendicular to the diffusing direction (Ref 15).

Sources of Error

Only sources of error which are believed to be greater than 1% are discussed at any length in the following paragraphs. Neglected, for instance, is a consideration of temperature and time variations due to heating and cooling of the furnaces used in the diffusion anneals. Since the only successful anneals were conducted in vacuum annealing furnaces, a qualitative glance at the factors involved will show that heating and cooling times were negligible. The maximum time required to heat the furnace to anneal temperature was the 1750°C. run in the ABAR furnace. Time to temperature was less than 15 minutes (0.25 hours). Time to cool to below 750°C. was less than 5 minutes (0.08 hours). This implies an error in time of some 0.33 parts in 188.9 (diffusion anneal time), or negligible as far as this paper is concerned. Similar analysis reveals temperature variations due to furnace heating and cooling were also insignificant.

Chemical Analysis. The chemical analysis of the microprobe standards is considered to be accurate to 1%. Density measurements of the standards were accurate to better than 1 part in 1000. The back-reflection method of measuring lattice parameters

is nominally accurate to better than .01% with good patterns and accurate extrapolations (Ref 9). Care was taken in this paper to insure that this accuracy was exceeded (Appendix C).

Microprobe Analysis. As outlined in the literature, quantitative analysis of binary alloys by microprobe analysis can produce results of less than 1% error (Refs 4; 5; 6; 24; 27). Examination of the raw data on the diffusion zones submitted by the Advanced Metals Research Corporation (Appendix D) shows the concurrent V and Cb analyses done in traversing the diffusion zones differ by less than 2% for the extreme cases (i.e., a/o V + a/o Cb = 100 a/o ($\pm$ 2 a/o)). Maximum error from the microprobe analysis can conservatively be called 2%.

Temperature Variations. Differentiation of Equation (17) with respect to T, replacing the differentials with differences, and dividing by the original expression yields:

$$\Delta D/D = \frac{Q}{R}\left(\frac{\Delta T}{T^2}\right) \qquad (23)$$

Letting Q be 78,000 calories per mole, which is the maximum activation energy found for the diffusion of Cb in V (Table III), it can be seen that the errors for the temperature variations experienced during the diffusion anneals can run from a maximum of 26% for

the 1404°C. (± 21°) anneal to 9.1% for the 1750°C. (± 10°) anneal. A closer examination of the temperature variations mitigates this possible error.

A temperature recording of the 1400°C. anneal showed an almost perfect sinusoidal temperature variation of ± 21° about the equilibrium temperature with a period of 24 hours. Random temperature samplings taken throughout the other diffusion anneals showed a similar diurnal variation. Assuming this sinusoidal variation did in fact exist for all the runs, the effect of the temperature variation would tend to "cancel" most of the errors associated with the maximum fluctuation encountered. Assuming further that the time at the maximum deviation from the mean temperature was the same both above and below the mean equilibrium temperature as was documented in the 1404°C. run, the exponential effect of the temperature dependence of D would result in an error of 5% in D for the 1404°C. case and less for the higher temperature anneals. Based on the previous argument, it is the opinion of the author that an error of 5% is a reasonable figure for temperature errors in D. Temperature variations were the greatest single cause of experimental error.

Computer Solution of Matano Method. As discussed at length in Appendix D, the computer solution of the

Matano method for finding D is directly and particularly responsive to an accurate curve fit to the raw concentration gradient data. Care was taken to carefully find the curves that most closely fit the concentration-penetration data in probability coordinates so to reduce regenerated curve errors to a minimum. One point on the 1404°C. anneal couple regenerated curve differed from the raw data by 6.9%. The second greatest error was 3% for a point on another curve. All other errors averaged less than 1% with maximum differences less than 2% in all cases. For both the 6.9% and 3% errors in curve fit, the computer program did not calculate diffusivities due to excessive changes in curve slopes at those particular points. Therefore, all calculated diffusivities can be said to have less than 2% error due to the computer program.

Summary. In conclusion, the foregoing discussion has listed the four major causes of experimental error in this thesis. A major possible source of error not discussed here, but mentioned in Section II, is that of molal volume correction. This has been eliminated by running a parallel set of analyses with distances measured in atomic lattice parameters.

Therefore, it is believed that the results presented in this thesis have an uncertainty of less than 10%.

Diffusion Mechanisms

The derived activation energies and frequency factors presented in Table III, coupled with the incomplete intrinsic diffusion coefficient data calculated from one set of marker movements indicate that diffusion takes place in the columbium-vanadium system by a vacancy mechanism.

As Huntington summarizes (Ref 13), diffusion mechanisms through a crystal lattice (bulk diffusion) are mainly limited to three alternate possibilities: interstitial diffusion, vacancy diffusion, and diffusion by direct interchange of atoms. In this particular study, the interstitial diffusion mechanism can immediately be ruled out because the relative sizes of the solute and solvent atoms prohibit their inhabiting the interstices of the crystal lattice without complete distortion of the lattice structure and resultant enormous energy expenditures.

The direct exchange mechanism, and this includes Zener's "ring-diffusion" mechanism, requires that there be no net displacement of atoms relative to the crystal lattice (Ref 19:302). In other words, the observance of a Kirkendall effect forbids the

employment of a direct exchange mechanism. Since a Kirkendall effect was observed for at least one of the diffusion couples in the Cb-V system (and the returns still out on the other couples), this provides direct evidence against the direct exchange mechanism in the Cb-V system.

Recommendations

Further Studies. Only partial conclusions could be drawn from the data derived and calculated in Section IV of this thesis. None of the analyzed diffusion couples had been returned by the time this report was written. Extensive metallographic work should be done on the specimen's diffusion zones not only to locate the "missing" markers in the three other couples wherein they were placed, but also to examine the diffusion zones for evidence of porosity and other microscopic anomalies that would have a profound effect on the values of diffusivities derived. The behavior of some of the diffusivity curves strongly suggests a porosity effect similarly noted by Peterson in a like study (Ref 24). Also, grain sizes should be rechecked to insure grain boundary diffusion effects were negligible in the areas where the microprobe analyses were taken. Only after extensive metallographic examination and location of the additional

markers has been done and the findings analyzed can the overall results of this thesis be intelligently evaluated in the light of the apparent diffusion mechanisms that have taken place.

Equipment. The greatest cause of experimental error was the uncontrollable temperature variation inherent in the Powerstat power supply to the vacuum annealing furnaces. The current supplied the heating elements is presently at the mercy of the vagaries of the line current. The daily rhythmic variations of the line current and its effect on temperature in the furnace hot zone and subsequent diffusion coefficient errors have been discussed previously. For accurate diffusion work, a constant temperature (or one with minimum fluctuations) is mandatory (See Equation 23). Therefore, a furnace constant voltage power supply is necessary to make the degree of diffusion experimental error compatible with the precise analysis tools now available.

If studies of diffusion processes in refractory metal systems are to be accomplished again, furnaces with high time/temperature capabilities are needed. The Marshall furnace is unsatisfactory for anneals above 1500°C. The present vacuum furnaces have apparently reached the limit of their capabilities

for sustained high temperature anneals above 1700°C. The NRC furnace failed after 176 hours at 1505°C., and the furnace was kept going for 400 hours at 1404°C. only by constant checking. Heating elements were replaced each time the specimen was checked during that particular run. The ABAR furnace failed after some 180 hours at 1750°C., but this was because of V contamination of the heating elements.

Bibliography

1. Baluffi, R.W. "On the Determination of Diffusion Coefficients in Chemical Diffusion." Acta Metallurgica, 8:871-873 (Dec 60).

2. Barrer, Richard M. Diffusion In and Through Solids. Cambridge, England:Cambridge University Press (1956).

3. Birchenall, C.E. "Volume Diffusion - An Empirical Survey" Atom Movements. Cleveland, Ohio:American Society for Metals (1951).

4. Birks, L.S. "The Electron Probe: An Added Dimension in Chemical Analysis". Analytical Chemistry, 32-9:19A (Aug 60).

5. Castaing, Raymond. Application of Electron Probes to Local Chemical Crystallographic Analysis. Unpublished Doctorate Thesis, University of Paris, France (Jun 51). Translated by Duwez, Pol and Wittry, David B. for Department of the Army. Watertown Arsenal Laboratory Report WAL 142/59-7. Watertown 72, Mass.: Watertown Arsenal Laboratory (Dec 55).

6. Castaing, Raymond. "Microanalysis by Means of an Electron-Probe, Principle and Corrections." Electron Physics. Washington, D.C.:National Bureau of Standards Circular 527 (1954).

7. Castaing, Raymond. "Applications of the Electron-Probe Microanalyzer." Electron Physics. Washington, D.C.:National Bureau of Standards Circular 527 (1954).

8. Crank, J. The Mathematics of Diffusion. Oxford, England:Clarendon Press (1956).

9. Cullity, B.D. Elements of X-Ray Diffraction. Reading, Mass.:Addison Wesley Publishing Co. (1956).

10. Garret, H.J. and Brocklehurst, R.E. Tables of Interplanar Spacings Computed for the Characteristic Radiations of Copper, Molybdenum, Iron, Chromium, and Cobalt. WADC Technical Report TR 57-381, ASTIA Document Number AD 142344, Wright-Patterson AFB, Ohio:Wright Air Development Center (Feb 58).

11. Hansen, Max. Constitution of Binary Alloys (2nd Edition). New York:McGraw-Hill Book Co., Inc., 1022 (1958).

12. Hartley, Craig S. "A Computer Program for the Matano Analysis of Binary Diffusion Data." Journal of Metals, 14:95 (Jan 62). (Also to be published as W.A.D.C. technical report in 1962).

13. Huntington, H.B. "Mechanisms of Diffusion." Atom Movements. Cleveland, Ohio:American Society for Metals (1951).

14. Jedele, A. Zeitung fur Electrochemische, Vol 39: 691 (1933).

15. Jost, Wilhelm. Diffusion in Solids, Liquids, Gases. New York: Academic Press, Inc. (1952).

16. Kirkendall, E.O. and Smigelkas, A.D. "Zinc Diffusion in Alpha Brass." Transactions of the AIM(M)E, 171, (1947).

17. Klotz, Irving M. Chemical Thermodynamics. Englewood Cliffs, N.J.:Prentice-Hall, Inc. (1950).

18. le Claire, A.D. "Diffusion of Metals in Metals." Progress in Metal Physics, Vol. 1, edited by Bruce Chalmers. New York:Interscience Publishers, Inc., 308-376 (1949).

19. le Claire, A.D. "Diffusion in Metals." Progress in Metal Physics, Vol. 4, edited by Bruce Chalmers. New York:Interscience Publishers, Inc., 6 (1953).

20. Matano, C. "On the Relation Between Diffusion Coefficients and Concentrations of Solid Metals (The Nickel-Copper System)." Japanese Journal of Physics, 8:109 (1933).

21. Miller, George L. Tantalum and Niobium. New York: Academic Press, Inc. (1959).

22. Pearson, William B. A Handbook of Lattice Spacings and Structures of Metals and Alloys. New York: Pergammon Press (1958).

23. Peterson, Norman L. Diffusion in Refractory Metals. WADD Technical Report 60-793. Wright-Patterson AFB, Ohio:Wright Air Development Division, ARDC, USAF (Mar 60).

24. Peterson, Norman L. Diffusion in the Uranium-Niobium System. Unpublished Doctorate Thesis, Massachusetts Institute of Technology, Cambridge 39, Mass. (Aug 61).

25. Rapperport, E.J. and Hartley, C.S. "A Review of Diffusion in Refractory Metal Systems." Unpublished paper presented to AIM(M)E (Apr 62). To be published.

26. Rostoker, William. The Metallurgy of Vanadium. New York: John Wiley and Sons, Inc. (1958).

27. Schwartz, C.S. and Austin, A.E. "Microbeam Analyzer at Battelle Memorial Institute". Journal of Applied Physics, 28:1368 (1957).

28. Sherby, Oleg D. and Simnad, Massoud T. "Prediction of Atomic Mobility in Metallic Systems." Transactions Quarterly of the American Society for Metals, 54-3:227-240 (Sept 61).

29. Smithells, Colin J. Metals Reference Book, Vol II. New York:Interscience Publishers, Inc. (1955).

30. Van Vlack, Lawrence H. Elements of Materials Science. Reading, Mass.:Addison-Wesley Publishing Co., Inc. (1960).

31. Wilhelm, H.A., Carlson, O.N., and Dickinson, J.M. "Columbium-Vanadium Alloy System." Transactions of the AIM(M)E (Aug 54).

32. Wells, Cyril. "Chemical Techniques and Analysis of Diffusion Data". Atom Movements. Cleveland, Ohio: American Society for Metals (1951).

Appendix A

Electron Microbeam Probe

General. A coherent study of diffusion data for a binary metallic system is dependent on complete and accurate analysis and interpretation of concentration-penetration data as outlined in Section II of this thesis. Numerous techniques exist that can be used to determine concentration gradients present in diffusion zones. However, none of these standard techniques possess the precision or resolution for proper analysis of zones containing steep chemical gradients or systems with very narrow diffusion zones (Refs 29:549; 25).

The electron microbeam probe technique developed by Castaing is a relatively new micro-chemical analysis which has demonstrated ability to measure the chemical composition of very small volumes of material (Refs 5; 6; 7). Briefly, the technique is described as follows: An electron beam is focussed to a diameter of about one micron on the region of the specimen from which a chemical analysis is desired. The penetration depth of the electrons is the order of one micron and therefore the back-scattered X-ray spectrum which results originates within a few millionths of a microgram of material. The chemical analysis derived from

the x-ray intensity data has the nominal precision of about ± 1% for binary alloys. However, to achieve this accuracy, intensity data of the binary must be available as a function of alloy composition (Refs 24; 5; 6; 7; 27). A general description of the theory and construction of the electron microbeam probe is presented below.

Diffusion zone electron micro-probe analysis was done for this thesis under Air Force contract by the Advanced Metals Research Corp., Somerville 45, Mass.

Introduction. The possibility of obtaining a chemical analysis by x-ray emission spectrography was first described by Moseley in 1913. He showed that when an element is bombarded by an electron beam a spectrum of wave-lengths characteristic of the element is emitted. However, the problems of focussing the electron beams and necessary power supply stability remained as obstacles to exploitation of this principle. During the development of electron microscopes in the late 1930s and early 1940s, much work was done and knowledge gained to overcome these difficulties. The successful development of the first electron probe microscope was reported in a thesis by Castaing in 1951, and his efforts demonstrated the resolution

of the technique and the precise analyses possible (Refs 5; 6; 7).

General Description and Theory. In essence, the electron microbeam probe is a demountable x-ray tube that has its beam focussed to an area of about one square micron (10^{-3} mm)^2. In order to obtain an analysis from such a small area, it is necessary to utilize an extremely precise electron optical system to focus the electron beam at the surface of the specimen. The irradiated area then emits an x-ray spectrum that is composed of the specimen's characteristic lines and a continuous spectrum. The intensity of the characteristic lines are proportional to the amount of the element present, and the total energy of the continuous spectrum is proportional to the average atomic number of the irradiated area. Details of design and construction of various electron probes are available in the literature (Refs 5; 6; 7; 24; 27).

The five essential components of the electron microbeam probe are:

1. The electron optical system which consists of an electron gun assembly and electron lenses which focus the electron beam on the surface of the specimen.

GA/MECH 62-2

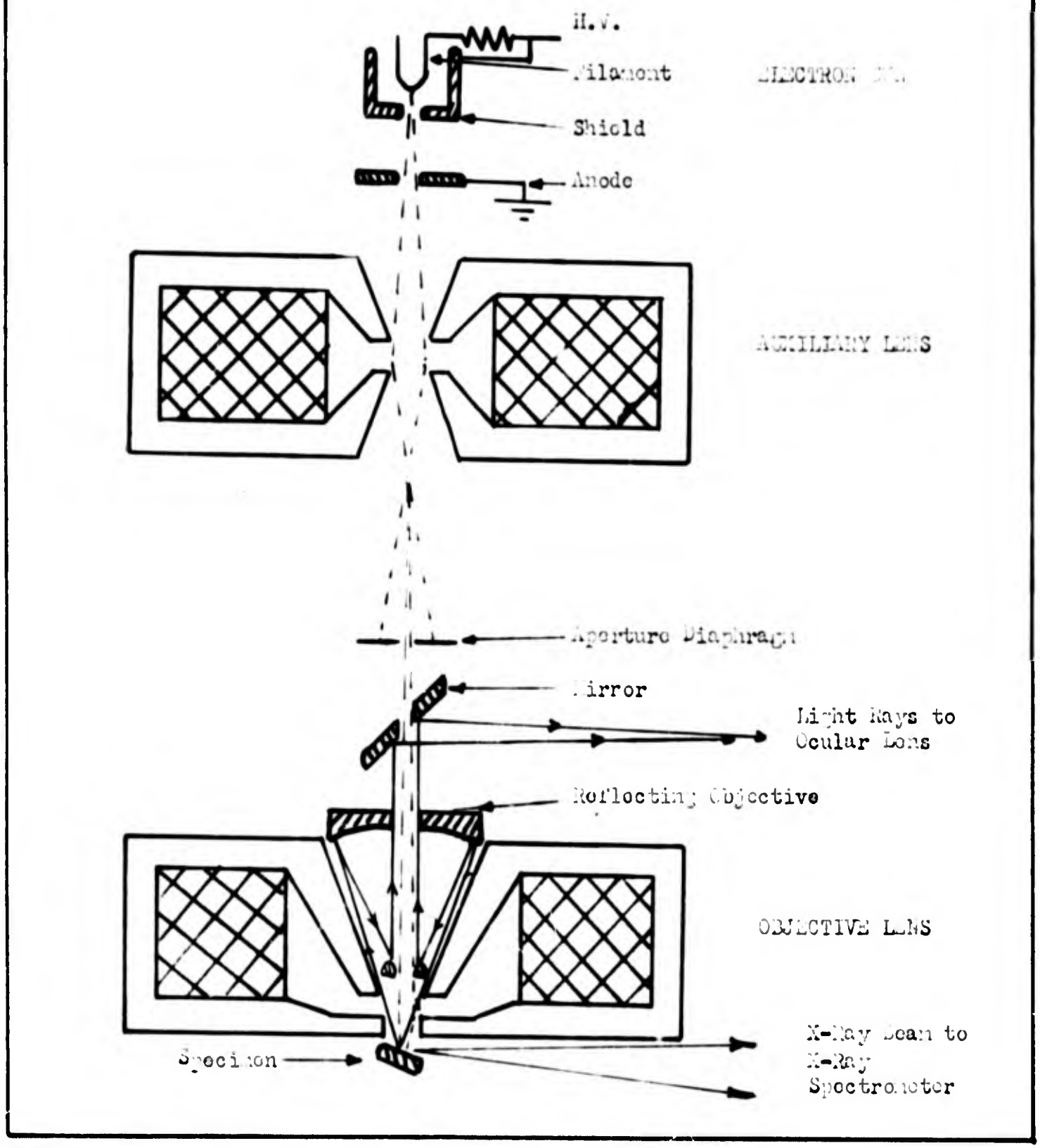

Figure 21- Schematic Drawing of Electron Microbeam Probe

2. A light optical system for viewing the specimen.

3. A mechanical translation system for accurately moving the specimen so that analyses of desired regions can be made.

4. A crystal spectrometer and x-ray detection equipment for analyzing the spectrum emitted by the bombarded area.

5. Electrical power and vacuum sources.

The first four of these basic components are illustrated schematically in Figure 21. The electron optical system is the most complex of the basic components.

The electron microbeam probe consists of an electron gun, which supplies electrons from a hairpin filament, followed by one or more electron lenses which may be magnetic, electromagnetic, or electrostatic. The probe is obtained by forming a reduced electron image of the cathode on the surface of the specimen. The size of this image may vary from 0.1 to 5.0 square microns depending on the quality of the electron optical system. Since the abovementioned components are found in any electron microscope, many probes have been built based on the electron microscope as the basic unit (Ref 7).

When high energy electrons strike a material, some electrons are decelerated abruptly giving off

the familiar continuous radiation of the x-ray spectrum and some knock out tightly bound electrons of the target giving rise to a primary series of characteristic x-rays. Also, some of the high energy electrons are slowed down gradually by inelastic collisions with the electrons of the material and dissipate their energy as heat, and some electrons have elastic or inelastic collisions with atoms near the surface of the specimen and are backscattered out of the specimen. Low energy backscattered electrons are also produced by interactions with loosely bound electrons of the surface atoms. It is the primary series of x-rays which are a function of target composition, and they may be used to obtain quantitative compositional data on a binary system for which the constituents are known by comparing the intensities of the characteristic x-rays. By proper choice of crystals, counters, and wavelengths, it is possible to obtain extremely good sensitivity with the microbeam probe. Detection of 100 parts per million of a given constituent is fairly common, and quantitative analyses of binary alloys have produced results of less than 1% error (Ref 4).

GA/MECH 62-2

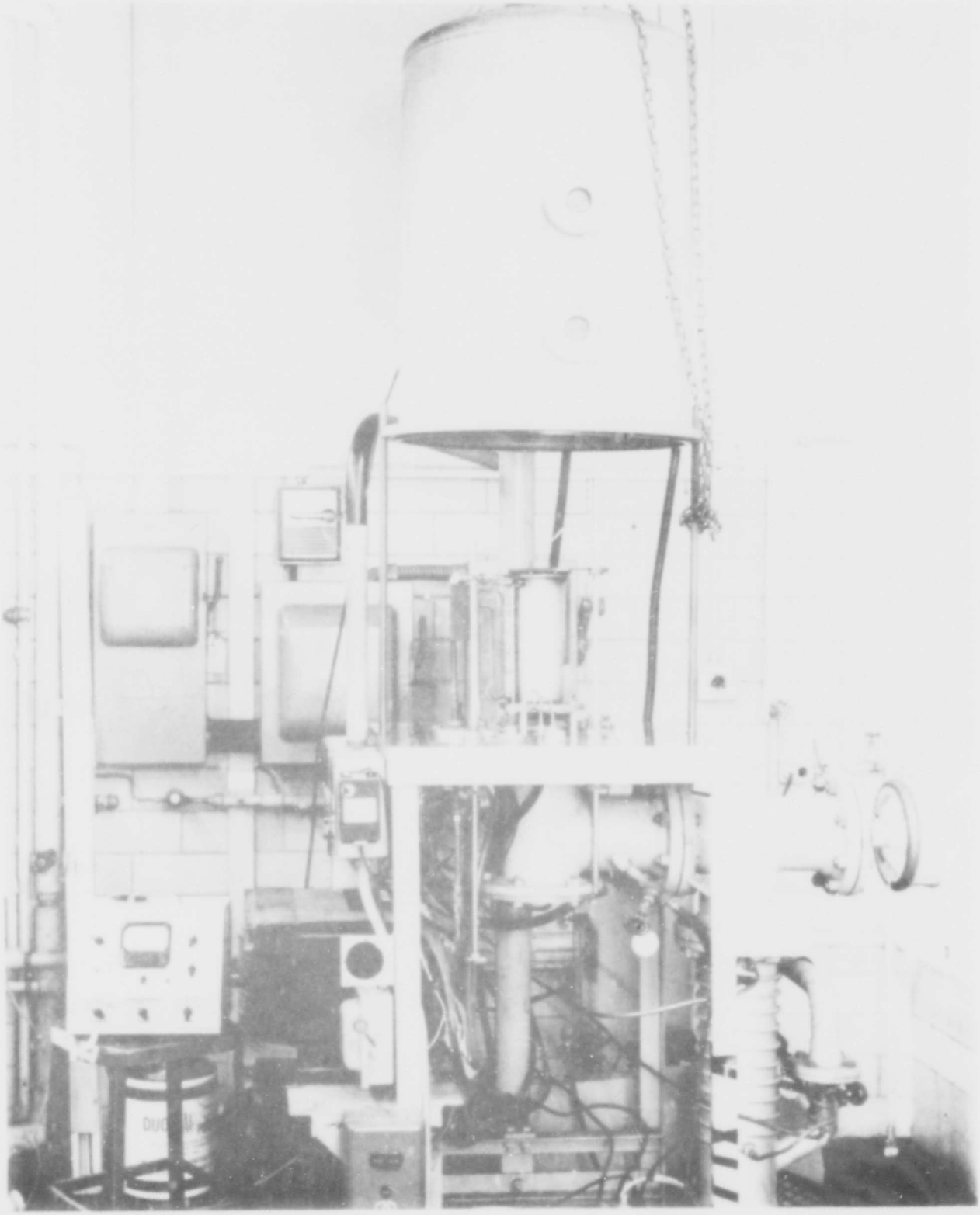

Figure 22 - View of NRC furnace. Stainless steel "bell" is in raised position showing heating element and thermocouple in position.

BLANK PAGE

Appendix B

General Equipment Description

This section is presented to briefly describe the furnaces used in the heat treatment of the diffusion couples, the attendant temperature measuring equipment, and the gas train used for purifying the inert gas shield used with the Marshall furnace.

NRC Vacuum Annealing Furnace

The National Research Corporation vacuum annealing furnace was used for the three hour bonding anneals of the diffusion couples, and the 1400, 1500, and 1600°C. diffusion anneals. In substance, the NRC furnace consists of a high-temperature tantalum-sheet heating element forming a hot zone 12 inches long and 3 inches in diameter mounted in a vacuum chamber. The vacuum chamber is formed by a large 24-inch diameter, 30-inch high, stainless steel, water cooled bell jar. It is designed to operate up to 2000°C. at a dynamic vacuum of 10^{-5} mm Hq (0.01 microns) pressure. Its general configuration is shown in Figure 22.

The pumping system incorporated into the furnace system consists of a high vacuum mechanical forepump (Kinney Single Plunger (VSD) Pump) in series with an oil diffusion pump (NRC Type H-6-P). Continuous

GA/MECH 62-2

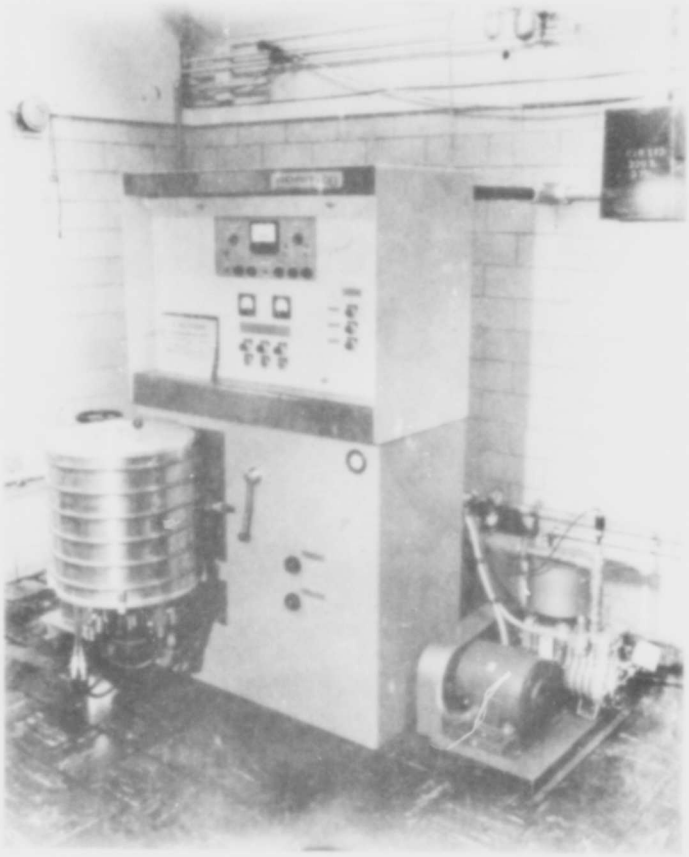

Figure 23 - View of ABAR furnace. Vacuum heating chamber is at left center, control panel is center, and mechanical pump is at lower right.

dynamic pressures of less than 0.05 microns were realized on all runs.

Temperature control was manual through a Powerstat power supply. At low temperatures (1400°C. and below), a platinum-platinum 10% rhodium thermocouple placed directly on the specimen being heat-treated provided continuous temperature readings that were recorded on a Minneapolis Honeywell "Brown Potentiometer." A tungsten-tungsten 26% rhenium thermocouple provided temperature readings for the 1500 and 1600°C. anneals. The tungsten thermocouple was read through a Leeds and Northrup potentiometer. All diffusion anneals maintained their equilibrium diffusion temperatures to within 21°C. (±) after equilibrium was established. The deviations apparently resulted from daily variations of the input line current to the powerstat. The variations for the 1500 and 1600°C anneals were based on random temperature samplings taken throughout anneals.

ABAR Vacuum Annealing Furnace

An ABAR, Series 90, Model C7T6A30, high temperature vacuum furnace was used for the 1750°C. diffusion anneal. The furnace and operating controls are in one compact unit (Figure 23). The vacuum

chamber is cylindrical with a diameter of 18 inches and a length of 18 inches. Heating elements are tantalum sheet foil, and the internal radiation shields are tantalum sheet. Hot zone size is 4 inches by 4 inches by 7 inches. Vacuum is produced by a Kinney KD-30 mechanical forepump and a NRC H6-1500 oil diffusion pump. Average vacuum during the diffusion anneal was 0.005 microns. Temperature was manually controlled through a Powerstat power supply. A tungsten-tungsten 26% rhenium thermocouple placed on the diffusion specimens provided temperature read out in the hot zone. Variations of temperature during the anneal did not exceed $\pm$ 10°C. after equilibrium was established. This was based on random temperature samplings taken throughout the anneal.

Marshall Tubular Furnace

A Marshall tubular furnace, internally wound with a platinum wire heating element, was used for homogenization anneal of the standard alloy specimens and three 1600°C. diffusion anneal attempts. In each case, the furnace was used in conjunction with a helium purifying gas train that is described later in this Appendix. The Marshall furnace described

GA/MECH 62-2

Figure 24 -Marshall Furnace in operation. Note ends of liner tube and controller. Gas train in right center background.

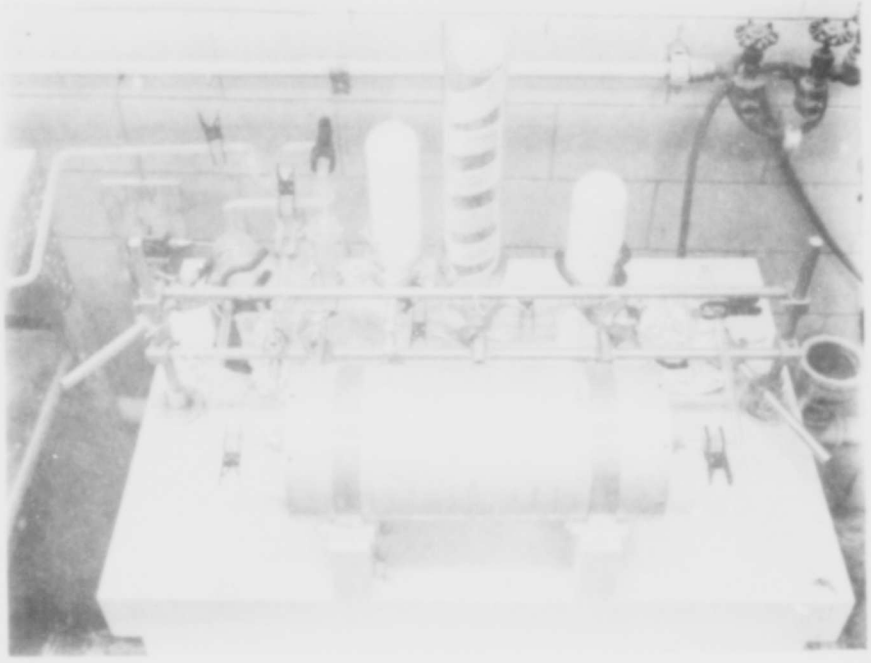

Figure 25- Inert gas purification train. Helium enters train center rear and leaves for gas inlet to furnace at left rear of photograph.

BLANK PAGE

here uses a platinum-50% rhodium heating element, and is designed for use up to 1700°C. The furnace is 20 inches long, and is mounted on a metal and asbestos sheet work table (Figure 24).

Necessary associated equipment with the furnace was a 1½ inch diameter mullite furnace tube liner fitted with glass extension ends. The glass extension ends were designed to permit thermocouple leads, gas tubing, and positioning rod outlets at either end to be passed through fitted glass or brass end plugs. The equipment worked satisfactorily up to 1300°C. However, all attempts at a diffusion anneal at 1600°C. met with catastrophic liner failure from 0 to 200 hours at temperature.

Temperature control was accomplished by means of a platinum-platinum 10% rhodium thermocouple mounted in the furnace thermocouple well and attached to a Leeds and Northrup "Micromax" controller. A second platinum thermocouple was hopefully placed in the center of the furnace hot zone at the proposed location of the specimens, and attached to a potentiometer. Invariably, either thermal shock or some other unknown reason caused rapid failure of this thermocouple.

GA/MECH 62-2

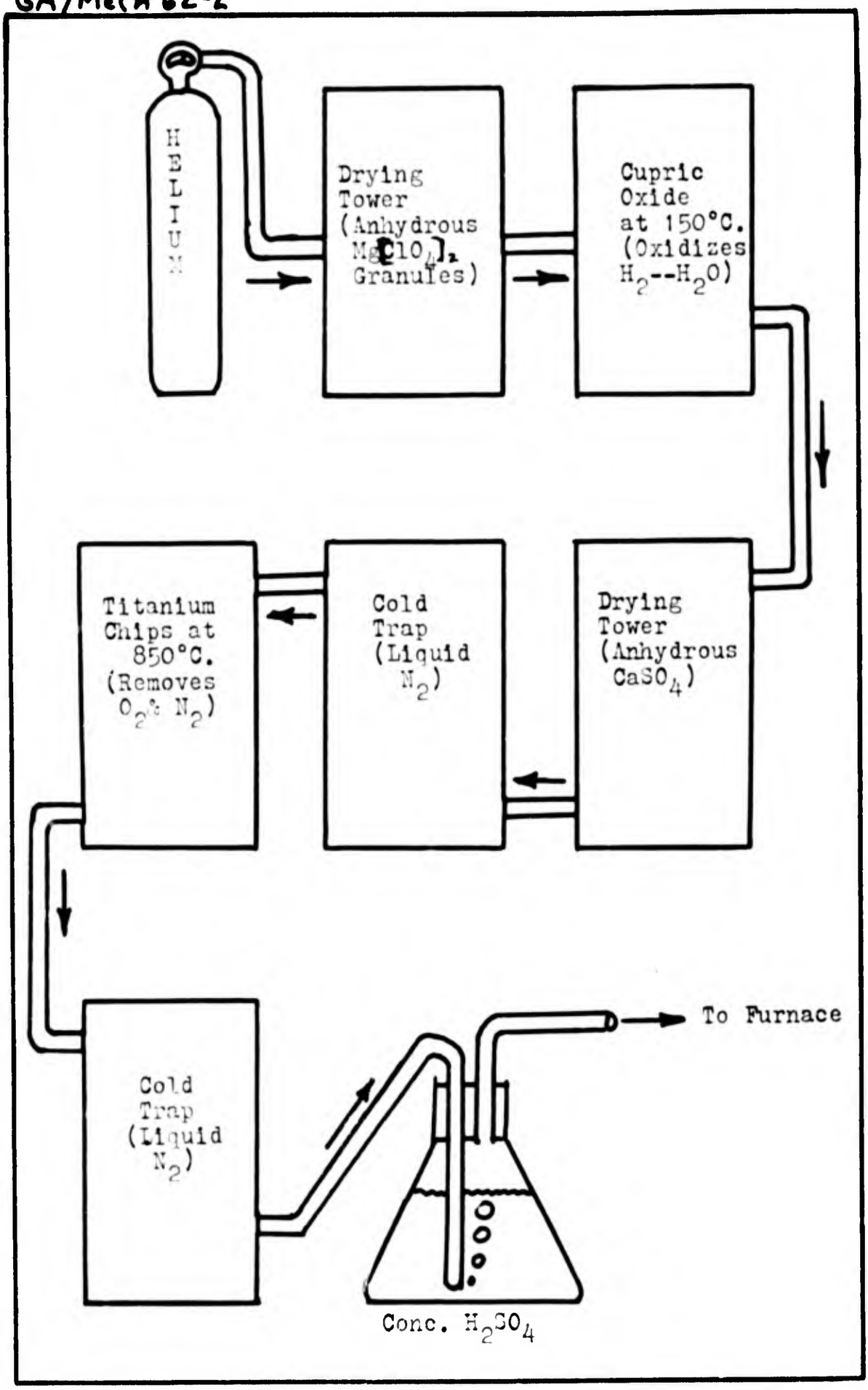

Figure 26 Schematic of Inert Gas Purification Train

Gas Purification Train

All the runs in the Marshall furnace required an inert gas shield to prevent specimen deterioration at temperature. Commercial tank helium was the gas source; however, the commercial grade of helium contains appreciable amounts of O_2, H_2O, and H_2 gas. The purification scheme employed is shown in Figure 25, and depicted schematically in Figure 26. As can be seen from the latter figure, provisions were made for removal of all suspected impurities.

Appendix C

X-Ray and Density Data

Actual atomic percentage determinations of the standards to be used in conjunction with electron microprobe analysis was done by a combination of lattice parameter measurements and density determinations as outlined in Section III. Total data derived are outlined and listed in this Appendix. All experimental work was done by the author.

X-Ray Data

The basic x-ray calculations were made using the general Bragg equation:

$$n\lambda = 2 d \sin \theta \qquad \text{(C-1)}$$

where d is the interplanar spacing of the specimen, λ is the incident beam wave length, n is an integer, and θ is the diffraction angle. Expansion of (C-1) yields:

$$n\lambda = 2 a \sin \theta / \sqrt{h^2+k^2+l^2} \qquad \text{(C-2)}$$

where a is the lattice parameter of the metallic crystal, and hkl are the indices of the reflecting crystal planes.

A summary of derived data from x-ray analysis of the standard specimens is presented on the

following pages. All data were taken by a Norelco 60-mm radius symmetric focussing back-reflection camera. The radiation was furnished by a copper target x-ray tube with a nickel radiation filter at power settings of 35 kilovolts and 19 milliamperes. The radiation wavelengths were then: $K\alpha_1$= 1.54050 angstroms, $K\alpha_2$=1.54434 angstroms, and the unresolved $K\alpha$ =1.54178 angstroms. In the data summary, the line column refers to one of these incident radiations. The powdered standard specimens were mounted on cellophane tape and placed in position so as to closely follow the circumference of the camera and thus prevent misalignment or displacement errors. The lattice parameter temperature was the temperature of the mounted specimen on the camera during exposure and was 28°C. for all runs. Angular measurements were made directly on the exposed film using fiducial marks incorporated on the circumference of the camera. This technique precluded film shrinkage errors. Interplanar distance, d, in angstroms (10^{-8}cm), for each set of lines was derived for a given 2θ value from WADC Technical Report 57-381 (Ref 10). Exposure times varied from two hours at the C_b end of the solid solutions to three hours at the V end. Derived values of the lattice

parameters, a, for each specimen were linearly extrapolated versus $\phi\tan\phi$ (where $\phi = \pi/2 - \theta$) by the method of least squares to $\phi = 0$. A sample calculation is included below for Specimen 9.

A least squares 2nd degree equation of lattice parameter variation as a function of composition is:

$$a_o = 3.0322 + 3.61 \times 10^{-3} (X) - 9.145 \times 10^{-6} (X)^2 (C\text{-}3)$$

where X is a/o Cb.

Sample Calculation. After the method outlined by Cullity (Ref 9:11-6), the normal equations of the a versus $\phi\tan\phi$ extrapolation are:

$$\Sigma a = \Sigma a_o + b \Sigma(\phi\tan\phi)$$

and,

$$\Sigma a(\phi\tan\phi) = a_o \Sigma(\phi\tan\phi) + b \Sigma(\phi\tan\phi)^2.$$

From the data presented for Specimen 9 (below), we have: $\Sigma\phi\tan\phi = 272.77$, $\Sigma(\phi\tan\phi)^2 = 20,704.8295$, $\Sigma a = 19.8210$, and $\Sigma a(\phi\tan\phi) = 901.3076$. Simultaneous solution of the two normal equations yields $a_o = 3.30234$ angstroms.

Table IV
X-Ray Data

Data for Specimen 1 (Nominal 0 a/o Cb)

Line	2θ (°)	d(angstroms)	hkl plane	a(angstroms)	$\phi\tan\phi$
$K\alpha_1$	123.35	0.875015	222	3.03114	35.8
$K\alpha_2$	124.29	0.873364	222	3.02542	81.7
$K\alpha_1$	143.64	0.810720	321	3.03344	26.0
$K\alpha_2$	145.10	0.809420	321	3.02857	24.3

Least squares extrapolation; $a_o = 3.03192$ angstroms

Table IV (Cont'd)

Data for Specimen 2 (Nominal 10 a/o Cb)

Line	2θ (°)	d(angstroms)	hkl plane	a(angstroms)	θtanθ
Kα	121.69	0.882856	222	3.05830	94.4
$K\alpha_1$	140.62	0.818083	321	3.06099	32.2
$K\alpha_2$	141.58	0.817700	321	3.05955	30.4

Least squares extrapolation; a_o = 3.06122 angstroms

Data for Specimen 3 (Nominal 25 a/o Cb)

$K\alpha_1$	135.66	0.831742	321	3.11209	43.2
$K\alpha_2$	136.43	0.831557	321	3.11401	41.5
$K\alpha_1$	164.22	0.777620	400	3.11048	4.4
$K\alpha_2$	166.17	0.777828	400	3.11123	3.4

Least squares extrapolation; a_o = 3.11067 angstroms

Data for Specimen 4 (Nominal 40 a/o Cb)

$K\alpha_1$	132.18	0.842555	321	3.15255	52.7
$K\alpha_2$	132.90	0.842325	321	3.15169	50.7
$K\alpha_1$	155.32	0.788466	400	3.15386	11.4
$K\alpha_2$	156.66	0.788468	400	3.15387	3.5

Least squares extrapolation; a_o = 3.15411 angstroms

Data for Specimen 5 (Nominal 50 a/o Cb)

$K\alpha_1$	129.53	0.851512	321	3.18607	59.9
$K\alpha_2$	130.54	0.850136	321	3.18092	58.0
$K\alpha_1$	151.01	0.795573	400	3.18229	16.1
$K\alpha_2$	152.26	0.795361	400	3.18144	14.5

Least squares extrapolation; a_o = 3.18148 angstroms

Data for Specimen 6 (Nominal 60 a/o Cb)

$K\alpha_1$	127.60	0.858448	321	3.21202	68.0
$K\alpha_2$	128.29	0.858061	321	3.21057	65.5
$K\alpha_1$	147.30	0.802711	400	3.21084	21.1
$K\alpha_2$	148.56	0.802173	400	3.20869	19.2

Least squares extrapolation; a_o = 3.20915 angstroms

Table IV (Cont'd)

Data for Specimen 7 (Nominal 75 a/o Cb)

Line	2θ (°)	d(angstroms)	hkl plane	a(angstroms)	ØtanØ
$K\alpha_1$	125.17	0.867696	321	3.24662	77.7
$K\alpha_2$	125.76	0.867554	321	3.24605	75.2
$K\alpha_1$	143.40	0.811280	400	3.24534	27.2
$K\alpha_2$	144.25	0.811334	400	3.24534	25.8

Least squares extrapolation; a_o = 3.24480 angstroms

Data for Specimen 8 (Nominal 90 a/o Cb)

$K\alpha_1$	123.29	0.875262	321	3.27493	86.3
$K\alpha_2$	123.79	0.875391	321	3.27541	84.0
$K\alpha_1$	140.05	0.819552	400	3.27821	33.6
$K\alpha_2$	140.80	0.819663	400	3.27865	32.0
$K\alpha_1$	172.80	0.771772	411	3.27435	0.9
$K\alpha_2$	174.49	0.773063	411	3.27983	0.5

Least squares extrapolation; a_o = 3.27753 angstroms

Data for Specimen 9 (Nominal 100 a/o Cb)

$K\alpha_1$	121.38	0.883300	321	3.30501	95.5
$K\alpha_2$	121.94	0.883120	321	3.30433	93.3
$K\alpha_1$	137.69	0.825910	400	3.30364	38.5
$K\alpha_2$	138.46	0.825840	400	3.30336	36.7
$K\alpha_1$	163.42	0.778383	411	3.30240	5.0
$K\alpha_2$	165.55	0.778350	411	3.30226	3.8

Least squares extrapolation; a_o = 3.30234 angstroms

Density Determination Data

The least squares linear (1st degree) equation of density as a function of a/o Cb is:

$$\rho = 6.09 + 24.4\times10^{-3}(X) \qquad \text{(C-4)}$$

where X is the atomic percentage of Cb. The density data is as follows:

Table V

Density Data

Specimen Alloy Number	Weight in air (gms)	Weight in H_2O (gms)	Density H_2O (gms/cc)	Density (gms/cc)
1	20.8874	17.4739	0.99788	6.106
2	13.1176	11.0216	0,99788	6.245
3	8.7839	7.4477	0.99788	6.560
4	14.3712	12.3261	0.99788	7.012
5	17.7944	15.3590	0.99788	7.291
6	18.1029	15.7101	0.99788	7.550
7	17.8182	15.5518	0.99790	7.845
8	15.1493	13.2973	0.99788	8.163
9	48.8663	43.1445	0.99788	8.522

Appendix D

Discussion of a Computer Program for the Matano-Boltzman Solution of Diffusion Data

General

Hartley has presented an IBM 7090 digital computer program which employs an error function curve fitting routine to raw concentration gradient data obtained from binary metal diffusion couples, and then calculates interdiffusion coefficients, D, using the Matano method (Ref 12). This program was used on all concentration-penetration data received from the microprobe analysis of the diffusion couples submitted to Advanced Metals Research Corp. for analysis. The following discussion is based almost completely on Hartley's work.

Three quantities must be found from an experimental concentration gradient in the diffusion zone to determine diffusivity at a point. First, the Matano interface must be established and thus determine the zero point of the abscissa. Second, the slope of the concentration-penetration curve must be measured at the concentration, C_n, for which the diffusivity is to be calculated. Finally, the area defined by the integral $\int_{C_i}^{C_m} x dC$ (See Figure 1) must be evaluated. All of these quantities are very

sensitive to the particular curve drawn through the experimentally derived points. In many cases, two apparently reasonable freehand curves through experimental points will yield slopes differing by a factor of two or more, and similar differences (to a lesser degree) in the location of the Matano interface and the measured area under the curve. Thus, the curve fit to experimentally obtained data is the key to analysis of diffusion data.

Hartley has summarized the empirical facts that concentration-penetration curves in many systems can be approximated to a high degree of accuracy by a series of 1st, 2nd, or 3rd degree curve segments on probability plots. That is, one in which the ordinate is linear in the argument of the cumulative normal distribution of the normalized concentration, and the abscissa is linear in distance x. By solving for the coefficients of these low order polynomials in probability coordinates, a concentration-penetration gradient can be reconstructed on cartesian coordinates. This method has the advantage that empirical observations have shown that the relation of the probability function of concentration to the distance x is generally a simpler one than that of C to x.

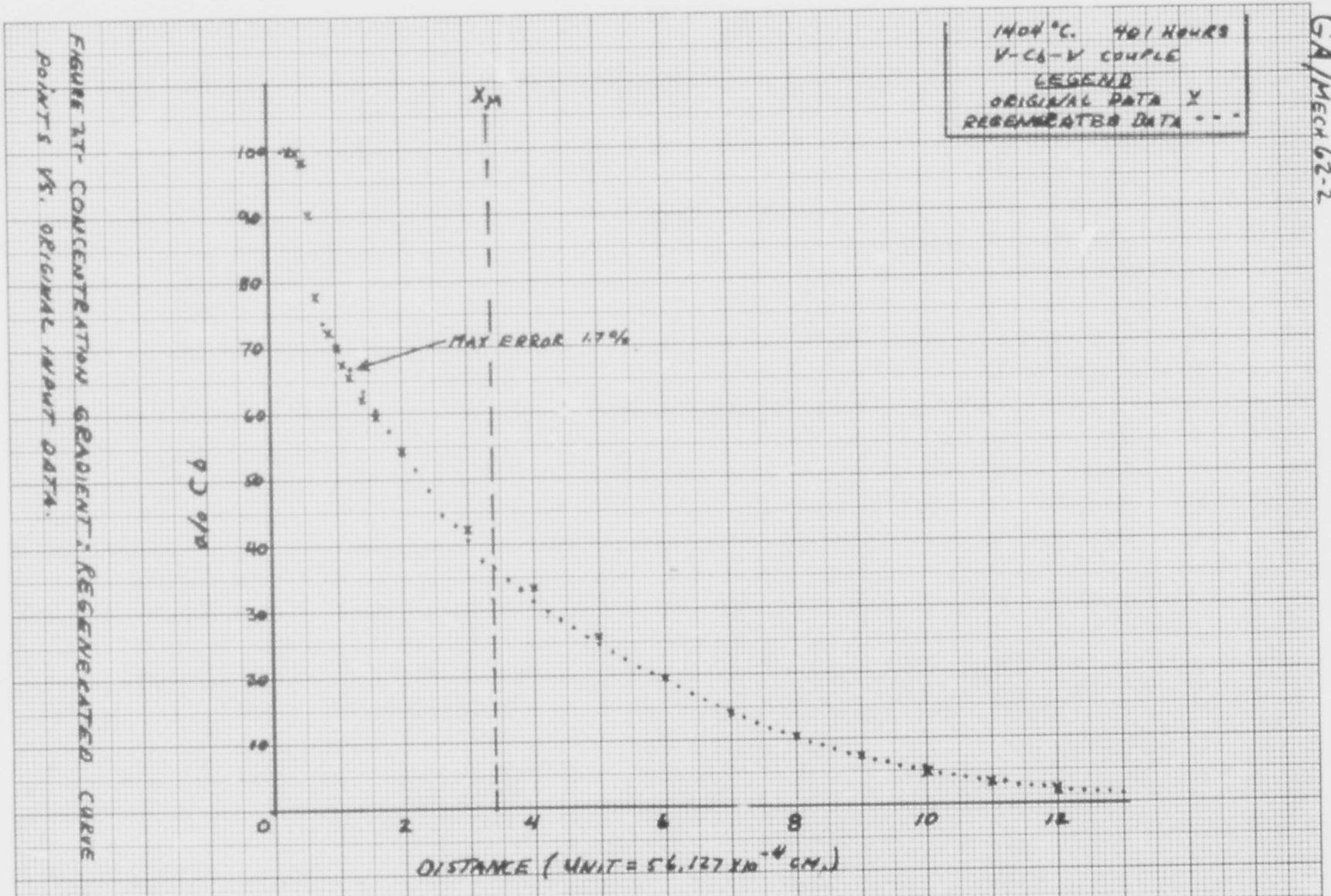

FIGURE 27 - CONCENTRATION GRADIENT: REGENERATED CURVE POINTS VS. ORIGINAL INPUT DATA.

FIGURE 27 - CONCENTRATION GRADIENT SHOWING REGENERATED CURVE POINTS VS. ORIGINAL INPUT DATA.

Therefore, in this computer program under discussion, the experimental data are used to construct a concentration curve by fitting a series of low order, least squares polynomials to a plot of concentration versus distance on probability paper. A new concentration-penetration curve, called the regenerated curve, is now calculated from these least square polynomials and tabulated in arbitrary equal distance increments (The intervals are usually smaller than the experimental data distance intervals). The new probability functions are then converted back to the original concentration units resulting in a regenerated concentration gradient in cartesian coordinates at equal distance intervals. The quality of this curve fit is checked by comparison with the original input experimental data - - the fit is considered good if the original data is reproduced to within experimental accuracy. A comparison of a regenerated curve with input data is presented in Figure 27.

The computer program then performs the Matano-Boltzman solution on this regenerated curve for arbitrary concentrations throughout the diffusion zone. For this particular analysis, 1 a/o intervals of concentration were used.

Input Data Preparation

The following three-step routine was performed on all sets of concentration-penetration data.

First, the raw data were plotted manually on probability paper to determine whether they were continuous and if they could be fitted with a smooth 1st, 2nd, or 3rd degree curve or combinations thereof. All data in this thesis were fitted with combinations of 1st or 2nd degree curves. Distance increments were converted to lattice parameter measure by means of Equation (C-3) and the same procedure followed.

Second, the raw data and the lattice parameter data were entered into the computer in tabular form. The computer was instructed to regenerate the data into a series of concentration-penetration curves (with equal distance increments as the ordinate) using the designated 1st or 2nd degree least squares fit of the raw data in probability coordinates. The error of each regenerated curve compared with the original data averaged less than 1%. There was a maximum error on one plot of 6.3% and another of 3%. However, in both these instances the diffusivity was not plotted at these points due to a discrepancy in slope calculation because of a rapidly changing curve slope. Maximum error was less than 2% in all other instances.

Finally, using the regenerated concentration gradient (now arranged in equal distance increments), the computer calculated the Matano interface and the interdiffusion coefficient using the Matano method outlined in Section II.

Table VI

Raw Data From Microprobe Analysis of Diffusion Specimens (Data furnished by Advanced Metals Research Corp., Somerville 45, Mass. Asterisk denotes concentration data used as computer inputs.)

I - Cb side of Cb-50-50 a/o alloy. 1750°C., 189 hours

Scan at 45° to interface. Unit step = 0.003125 ins.

Unit Steps	a/o V	a/o Cb (*)
0	49.0	51.0
1	48.9	51.2
2	48.5	51.5
3	47.8	52.0
4	47.2	53.0
5	46.6	53.5
6	45.7	54.1
7	45.0	55.0
8	44.0	56.0
9	43.0	56.3
10	41.9	57.6
11	41.0	58.8
12	39.5	60.0
13	38.0	62.0
14	36.4	64.1
15	33.5	66.5
16	31.0	68.5
17	28.2	71.1
18	25.4	74.3
19	21.9	77.5
20	16.5	83.9
20.5	12.5	88.5
21	6.5	92.8
21.5	2.1	96.0
22.0	0.3	99.2
22.5	-	100

II - V-Cb-V. 1404°C., 401 hours, 45° scan, unit step = 0.003125 in.

		(*)
0	0	100
0.2	0	100
0.4	0	99.8
0.5	2.3	98.0

Table VI (Cont'd)

II (Continued)

Unit Steps	a/o V	a/o Cb (*)
0.6	10.0	90.2
0.7	22.1	78.0
0.8	25.0	75.0
0.9	28.5	72.3
1.0	30.5	70.0
1.1	32.4	67.5
1.2	34.3	65.5
1.4	37.8	62.1
1.6	40.3	59.5
2.0	46.3	54.1
3	58.1	42.4
4	68.0	33.2
5	75.0	26.0
6	82.0	19.4
7	87.0	14.0
8	90.3	10.3
9	93.3	7.4
10	95.5	5.1
11	97.0	3.4
12	98.0	2.1
13	98.6	1.6
14	99.1	1.0
15	99.6	0.5

Further points not used

III - V side of Cb-50-50 a/o alloy-V. 1404°C, 401 hours, 45° scan, Unit step = 0.003125 ins.

	(*)	
0	100	0
1	99.8	0.2
2	99.7	0.3
3	99.5	0.4
4	99.0	0.8
5	98.3	1.0
6	97.6	1.6
7	96.6	3.0
7.5	96.0	3.6
8	95.1	4.3
8.5	94.2	5.0
9	93.1	6.2
9.5	91.6	7.3
10	89.9	10.0
10.5 (W-marker)	87.3	12.3
11	84.8	15.0

Table VI (Cont'd)

III (Continued)

Unit Steps	a/o V (#)	a/o Cb
11.5	82.0	18.0
12	79.0	21.3
12.5	76.0	24.0
13	73.2	26.7
13.5	70.5	28.8
14	67.9	31.1
14.5	66.0	33.4
15	64.0	35.5
15.5	62.0	37.3
16	61.0	38.8
16.5	59.6	40.5
17	58.7	41.6
17.5	57.8	42.7
18	57.0	43.5
18.5	56.7	44.1
19	56.0	44.3
19.5	55.7	44.5
20	55.6	44.5

IV - Cb side of Cb-50-50 a/o alloy-V. 1404°C., 401 hours. 45° scan, unit step = 0.001563ins

		(#)
0	55.2	44.5
0.5	55.2	44.7
1	55.1	45.0
1.5	55.0	45.2
2	54.7	45.4
2.5	54.5	45.8
3	54.1	46.0
3.5	53.4	46.5
4	53.0	47.0
4.5	52.5	47.5
5	51.8	47.9
5.5	51.1	48.7
6	50.3	49.5
6.5	49.4	50.5
7	48.5	51.3
7.5	47.3	52.8
8	46.6	53.4
8.5	45.5	54.5
9	44.0	55.6
9.5	43.1	56.3
10	41.7	58.1
10.5	40.6	60,0
11	39.0	61.0

Table VI (Cont'd)

IV (Continued)

Unit Steps	a/o V	a/o Cb (*)
11.5	37.8	62.2
12	36.0	64.5
12.5	34.0	65.8
13	31.8	68.0
13.5	29.0	71.8
14	26.0	74.0
14.5	22.0	78.0
15	15.5	84.8
15.3	8.0	92.2
15.5	3.0	97.0
15.7	1.4	99.0

Further points not used.

V - V-Cb-V. 1630°C., 190 hours, 45° scan, unit step = 0.003125 ins.

		(*)
0	0	100
0.5	2.5	97.2
0.6	7.5	92.7
0.7	12.0	89.0
0.8	17.5	82.5
0.9	20.0	79.9
1.0	22.0	78.1
1.2	25.5	74.6
1.5	29.0	71.0
2	33.7	66.8
2.5	37.5	62.2
3	41.0	59.0
4	47.5	52.4
5	53.0	46.5
6	58.8	41.2
7	64.1	35.8
8	69.1	31.3
9	73.6	27.0
10	77.1	23.1
11	80.5	19.5
12	83.4	16.6
13	86.0	13.8
15	89.8	9.5
17	92.6	7.0
19	94.6	4.8
21	96.6	3.3
23	98.0	1.7
25	99.0	1.0

Table VI (Cont'd)

V (Continued)

Unit Steps	a/o V	a/o Cb (*)
27	99.7	0.4
29	99.8	0.2
31	99.9	0.1

VI - Cb side of Cb-50-50a/o alloy-V, 1630°C., 190 hours
45° scan, unit step = 0.003125 ins.

	(*)	
0	53.7	45.9
1	53.5	46.5
2	52.8	47.3
3	52.3	47.8
4	51.8	48.9
5	51.1	49.6
6	49.7	50.4
7	48.3	51.2
8	46.6	53.4
9	44.7	54.8
10	42.2	57.0
11	40.3	59.2
12	38.1	61.0
13	35.6	63.6
14	32.7	66.5
15	29.7	70.1
16	25.8	74.0
16.5	23.7	76.3
17	21.1	79.2
17.2	19.8	80.6
17.4	18.2	82.1
17.6	16.0	84.0
17.8	13.8	86.1
18.0	10.6	90.0
18.1	8.8	92.0
18.2	4.8	94.1
18.3	2.3	97.0
18.4	0.4	99.2
18.5	0.0	100.0
18.6	0	100.0

VII - V side of Cb-50-50a/o alloy-V., 1630°C., 190 hours,
45° scan, unit step = 0.00625 ins.

	(*)	
0	100.0	0
1	100.0	0

Table VI (Cont'd)

VII (Continued)

Unit Steps	a/o V (*)	a/o Cb
2	99.9	0.1
3	99.8	0.2
4	99.8	0.3
5	99.5	0.6
6	98.8	1.1
7	98.3	1.8
8	97.2	2.6
9	96.0	3.9
10	94.5	5.3
11	92.4	7.1
12	90.0	9.7
13	87.0	12.8
14	83.2	16.2
15	79.2	20.9
16	74.7	26.6
17	70.0	30.7
18	65.7	36.4
19	61.4	38.0
20	57.4	41.1
21	55.4	44.0
22	54.1	45.9
23	53.7	46.2

VIII - V side of V-50-50a/o Alloy, 1505°C., 176 hours, 45° scan, unit step = 0.00625 ins.

	(*)	
0	100.0	0
1	99.9	0.1
2	99.8	0.2
3	99.4	0.4
4	98.8	0.9
5	97.4	2.7
6	94.7	5.4
7	90.0	10.0
7.5	86.7	13.0
8	82.7	16.7
8.5	78.7	21.3
9	73.0	26.6
9.5	67.9	32.6
10.5	59.8	40.2
11	57.0	43.1
11.5	54.6	45.3
12	53.0	47.0
12.5	51.8	47.8
13	51.5	48.5
13.5	51.5	48.5
14	51.5	48.5

Vita

Robert Charles Geiss was born [redacted] in [redacted]; the only child of indigent immigrant parents, Robert Hans Geiss and Bertha [redacted] Geiss. He was graduated from the Massachusetts Institute of Technology in June 1950 with a Bachelor of Science degree in Metallurgy. After working as a research metallurgist for Wright Aeronautical Corporation for a short time, he entered aviation cadet training in 1951, and was graduated as a Second Lieutenant and navigator in July 1952. His military assignments prior to this tour at the Institute of Technology included a combat tour as a B-29 crew member with the 19th Bomb Wing out of Okinawa during the Korean War, squadron navigator in the 44th Air Refueling Squadron, SAC, for 3 years, attendance and graduation from the aero-mechanical engineering program (1 year) at AFIT in 1957, and, finally, a 3 year tour as aircraft maintenance officer with the 1503rd ATW, MATS, Japan. He is married to the former Nancie [redacted] of Texas and has three children, Margaret, Robert, and Susan.

Permanent address: [redacted]

This thesis was typed by Miss Charlotte Yvonne Corder.